Enclosure 3

Exelon Report AM-2005-015, "A Comparison of the Cumulative Mean Square Strain in the Application of the Modified 930 MWe Acoustic Circuit Model and FEA to the QC2 TC41 In-Vessel Test Condition," Revision 0

A Comparison of the Cumulative Mean Square Strain in the Application of the Modified 930 MWe Acoustic Circuit Model and FEA to the QC2 TC41 In-Vessel Test Condition

Document Number AM-2005-015
Revision 0

Nuclear Engineering Department
Exelon Nuclear Generating Co.

Prepared by:	Kevin Ramsden	**Date:**	11/14/05
Reviewed by:	Guy DeBoo	**Date:**	11/14/05
Approved by:	Roman Gesior	**Date:**	11/14/05 (Date Issued)

Abstract

This report documents the comparison of predicted strain measurements and frequency response to plant measured strain data. The intent of this report is to assess the margins obtained when applying the Modified 930 MWe Acoustic Circuit Model (ACM) load definition in conjunction with the detailed Finite Element Model (FEM) for the evaluation of steam dryers subjected to unsteady pressure loads.

Abstract....2
1. Introduction....4
2. Description of Methodology....5
2.1 Strain Gage Measurements....5
2.2 Strain Gage Measurement Accuracy....5
2.3 Structural Analysis....5
3. Calculations/Data Considerations....6
3.1 Software Applications....6
3.2 Comparison of Modified 930 MWe ACM to QC2 Test Condition 41 Data ...6
4. Results....7
5. Conclusions/Discussion....24
6. References....25
Appendix A 26

1. Introduction

This report documents the comparison of cumulative mean square strain between the prediction and measurements of strain on the Quad Cities (QC) Unit 2 replacement steam dryer. The Continuum Dynamics, Inc. (CDI) Modified 930 MWe Acoustic Circuit Model (ACM) takes inputs from Main Steam Line (MSL) mounted strain gages and provides a detailed pressure time history for the steam volume of the reactor pressure vessel, with emphasis on the surfaces of the steam dryer. This methodology has been validated against in-plant dryer pressure measurements taken on the QC2 instrumented steam dryer during power ascension testing. The output of the ACM is used as input to the General Electric (GE) Finite Element Model (FEM), which is used to compute the stresses in the dryer for comparison against code allowable fatigue and stress limits.

This report examines the predicted strains for selected measurement locations on QC2 Test Condition 41 (TC41) and compares them with the actual measured data. These predicted strains are based on the use of the Modified 930 MWe ACM and the GE FEM. The intent is to assess the margin in the overall process used to calculate steam dryer unsteady pressure loads and their resultant effects on the steam dryer.

2. Description of Methodology

2.1 Strain Gage Measurements

The dryer-mounted strain gages used in this evaluation are:

S-1 Horizontally located on the skirt near 90° Azimuth

S-5 Closure plate location near 0° Azimuth

S-7 Top of Hood near 90° Azimuth

S-8 Skirt near 90° Azimuth

S-9 Front Hood near 90° Azimuth

Drawings showing the location of the strain gages are provided in the Appendix. Data was collected for these sensor locations at a frequency of 2048 samples per second during testing. This data is contained in the following file:

TC41-2_sg_ac.txt dated Monday, May 23, 2005, 1:33:18 PM

2.2 Strain Gage Measurement Accuracy

The measurement accuracy determination for the Kyowa strain gages mounted on the dryer, along with the loop accuracy is documented in Reference 1. The accuracy of the dryer mounted strain gages has been determined to be +/- 4.2% absolute error and 1.1% relative error. Because this evaluation considers a comparison of the cumulative mean squares of predicted strains to measured strains, it is appropriate to apply the absolute error term when considering the results.

2.3 Structural Analysis

The structural analysis (References 4, 5, and 6) is performed on a two-second interval of data selected from the ACM. The FEA is a direct integration solution and uses two-millisecond time steps. The computed time histories at the strain gage locations are then extracted. The time step size is varied +/- 10% to provide allowance for uncertainties in structural frequency. The FEA data was transmitted by Reference 7.

3. Calculations/Data Considerations

3.1 Software Applications

The Mathcad-11 software package was used to support this evaluation. The spectral analyses presented were performed using complex Fast Fourier Transforms (FFTs), to allow characterization of the frequency content and power spectral density (PSD) of the predicted and measured data.

3.2 Comparison of Modified 930 MWe ACM to QC2 Test Condition 41 Data

To generate these comparisons, the following sequence was applied:

1) The FEM time history was a two-second interval between 10.4 and 12.4 seconds, at a two millisecond time step.
2) The plant strain gage data was then reduced to match the same time interval and was sampled to provide similar time steps (every fourth point was taken, with the original data record frequency of 2048 Hz).
3) The PSDs were computed and then a frequency dependent series summation of the PSD coefficients, representing the integrated response, was calculated.

Performing the data manipulation in this manner provides an appropriate and equivalent comparison, and prevents having to manipulate the scaling inherent in the FFT process.

4. Results

Plots of cumulative mean square strains are presented in Figures 1-5 for the nominal cases, Figures 6-10 for the minus 10% cases, and Figures 11-15 for the plus 10% cases for each strain gage, respectively. The following observations are noted.

1) For the S-1 location on the skirt, predicted strains exceed measured strains by a factor of approximately 4.25.
2) The S-5 (closure plate) location is underpredicted in the nominal case, but overpredicted in both the minus 10% and plus 10% cases.
3) The S-8 location (skirt) is largely overpredicted by the FEM. The FEM exhibits a large increase at approximately 35 Hz; however, this response is an artifact of the FEM and is not replicated in the measured data.
4) For the S-9 location on the hood face, predicted strains exceed measured strains by a factor of approximately two.
5) The plots illustrate that there is minimal low frequency response in the plant measurements; the FEM also exhibits little response at low frequency, except for the response at 35 Hz for the S-8 location, as discussed above.
6) There is no evidence of any significant plant response to the 139 Hz signals observed in the dryer pressure data. S-5 is the only sensor displaying any response at this frequency, and that response is negligible relative to the 150 Hz response.
7) The FEM response shows a tendency to build significantly prior to reaching the 150 Hz point; this tendency is not reflected in the measured data. For example, the S-9 point shows a step increase near 90 Hz, which would match the calculated modal frequency for the hood.
8) The delta strain that occurs at 150 Hz is larger in the FEM than observed in the plant.
9) The plant data illustrates that most of the strain response occurs as a result of the 150 Hz loads.

Tables 1 through 3 provide a summary of the key elements of this comparison for the nominal, minus 10%, and plus 10% cases, respectively.

Figure 1 Cumulative Mean Sq Strain Comparison S-1 Nominal

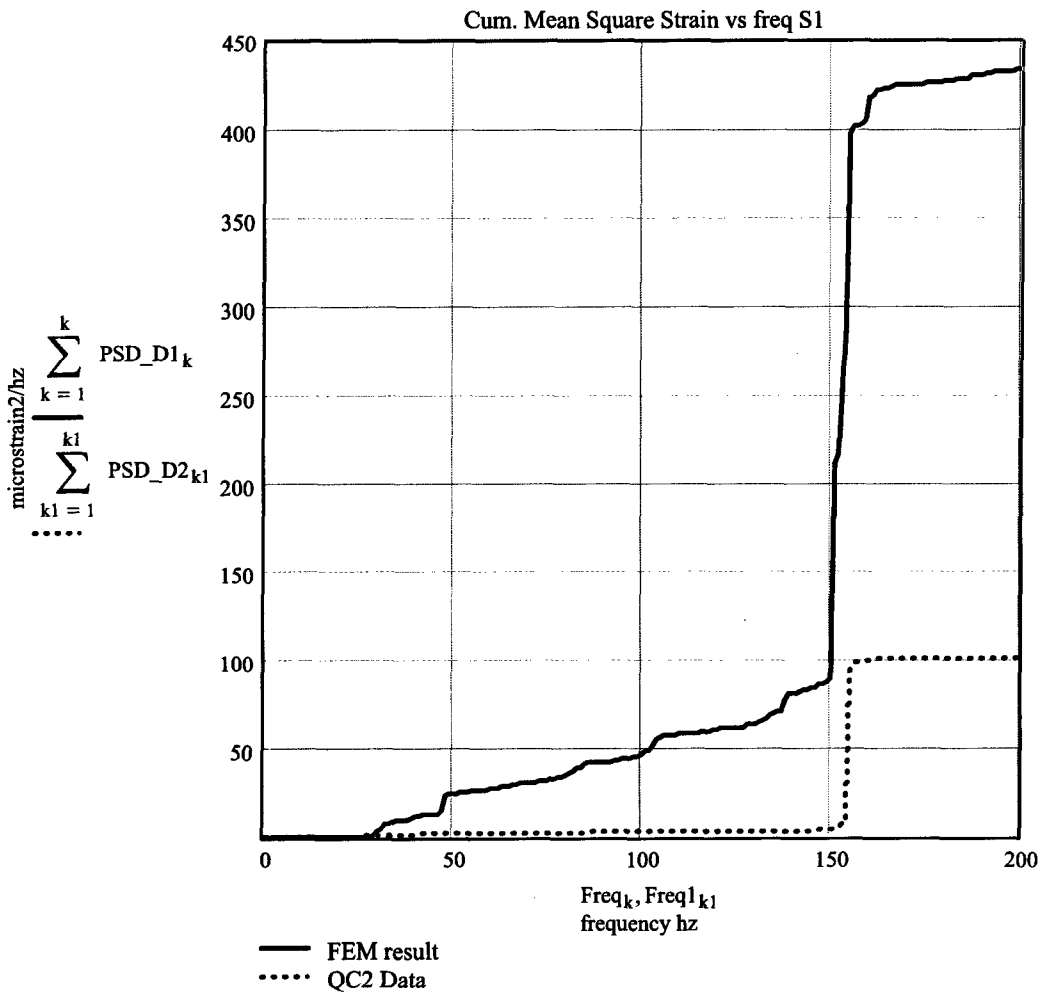

Figure 2 Cumulative Mean Sq Strain Comparison S-5 Nominal

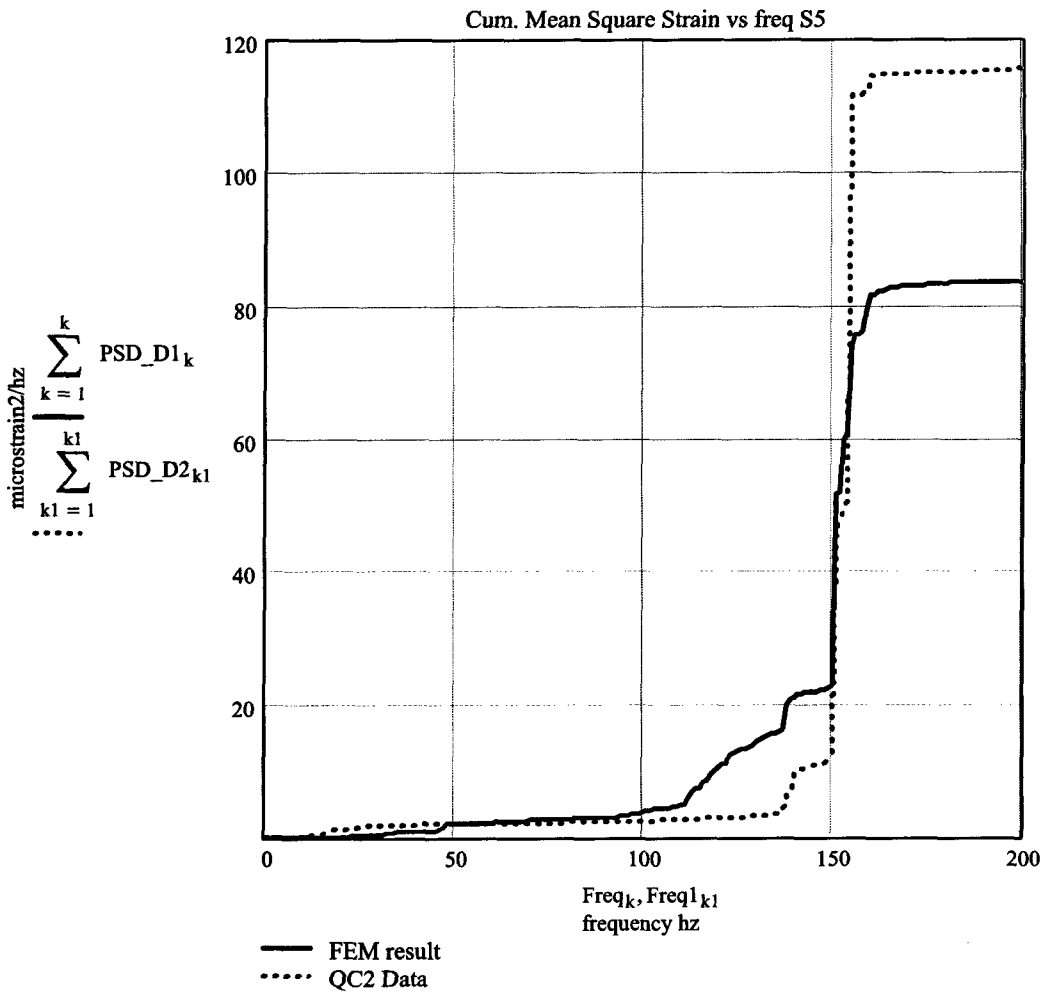

Figure 3 Cumulative Mean Sq Strain Comparison S-7 Nominal

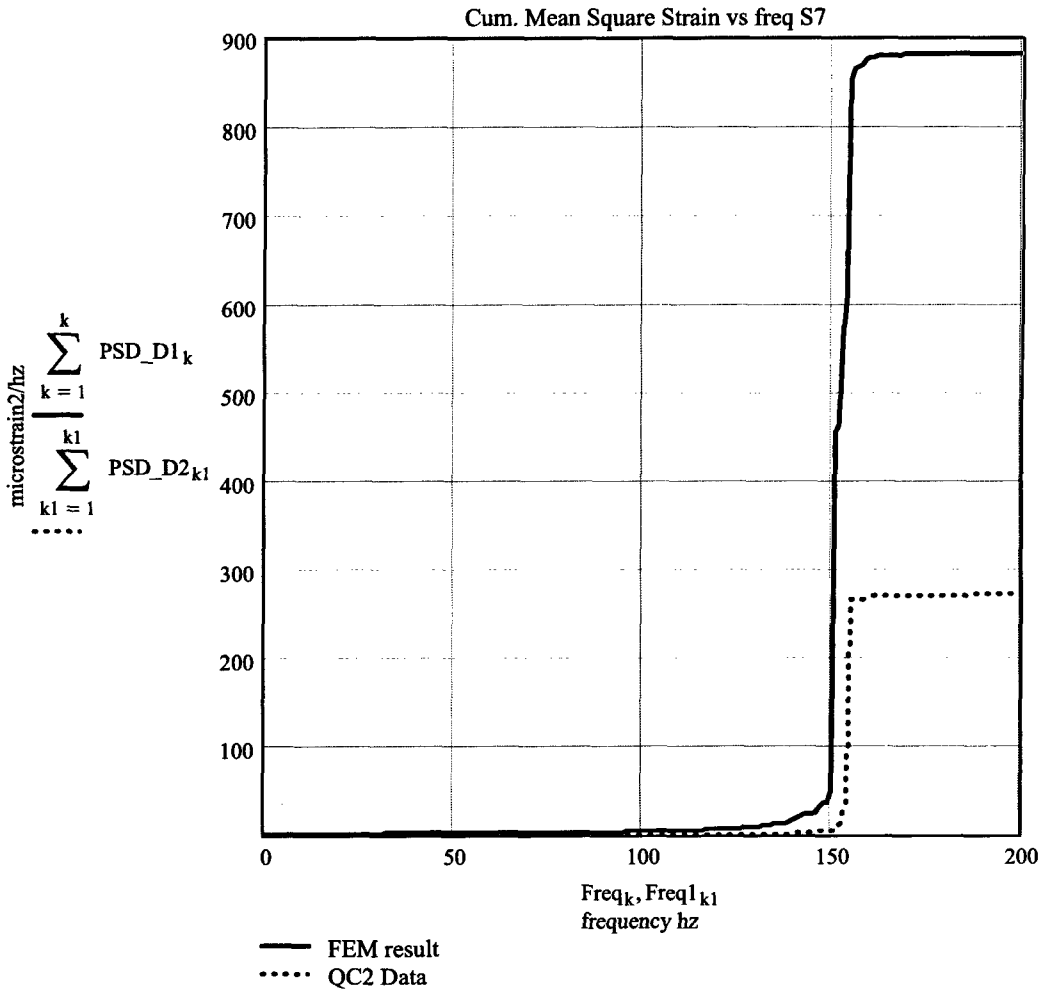

Figure 4 Cumulative Mean Sq Strain Comparison S-8 Nominal

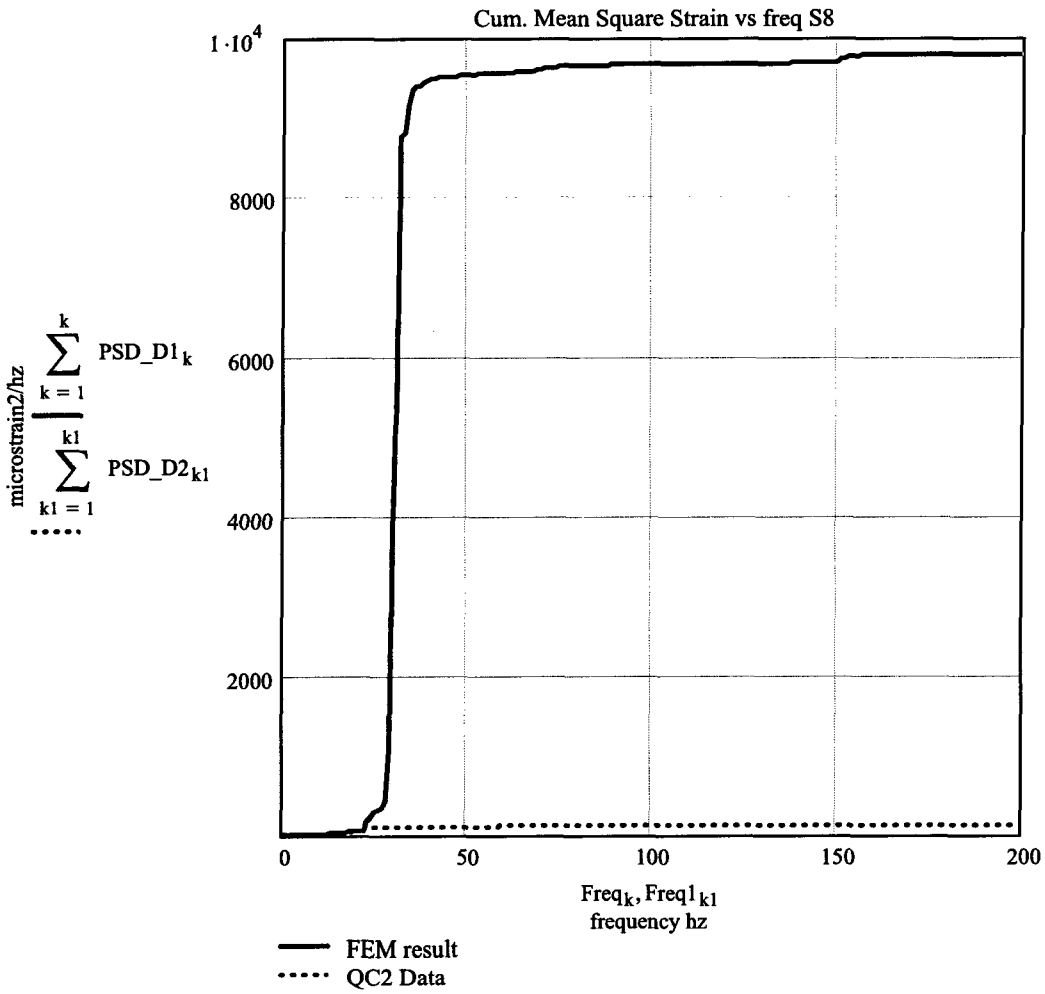

Figure 5 Cumulative Mean Sq Strain Comparison S-9 Nominal

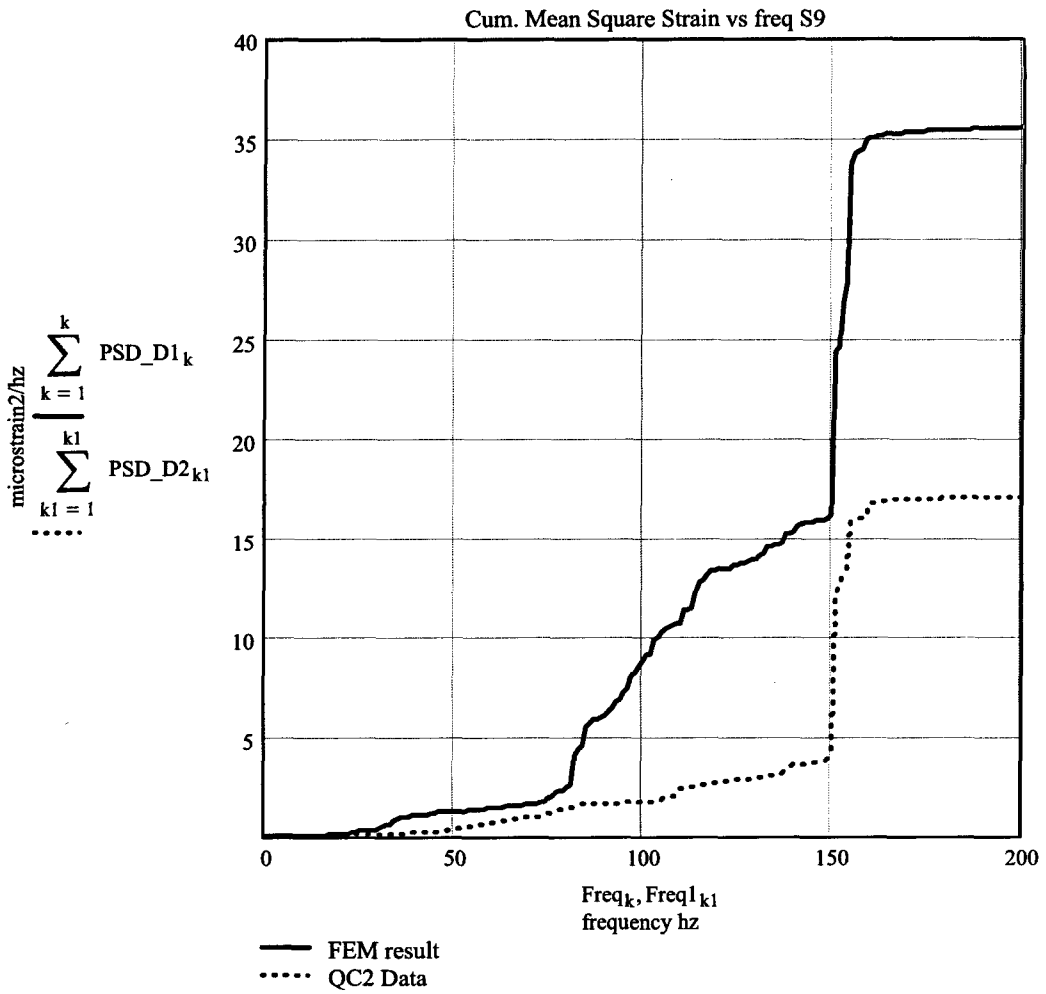

Figure 6 Cumulative Mean Sq Strain Comparison S-1 Minus

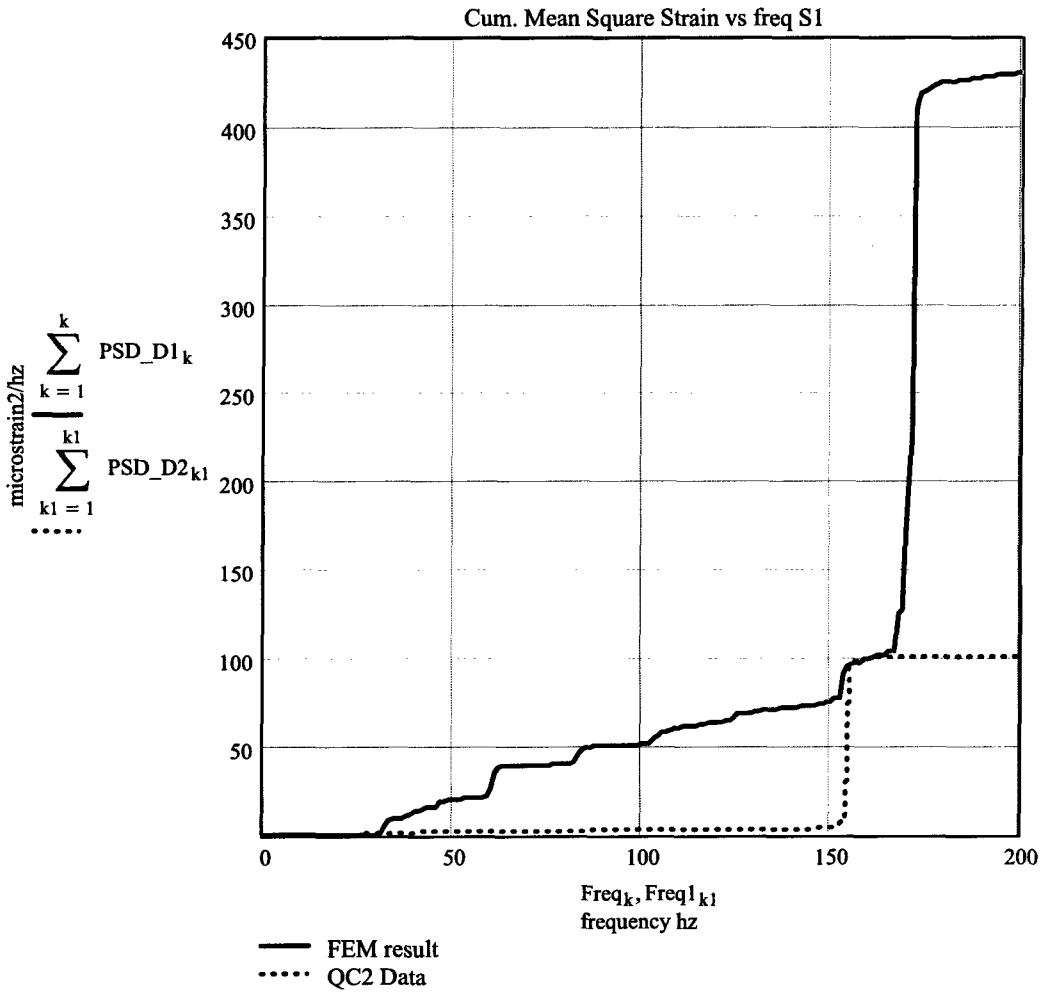

Figure 7 Cumulative Mean Sq Strain Comparison S-5 Minus

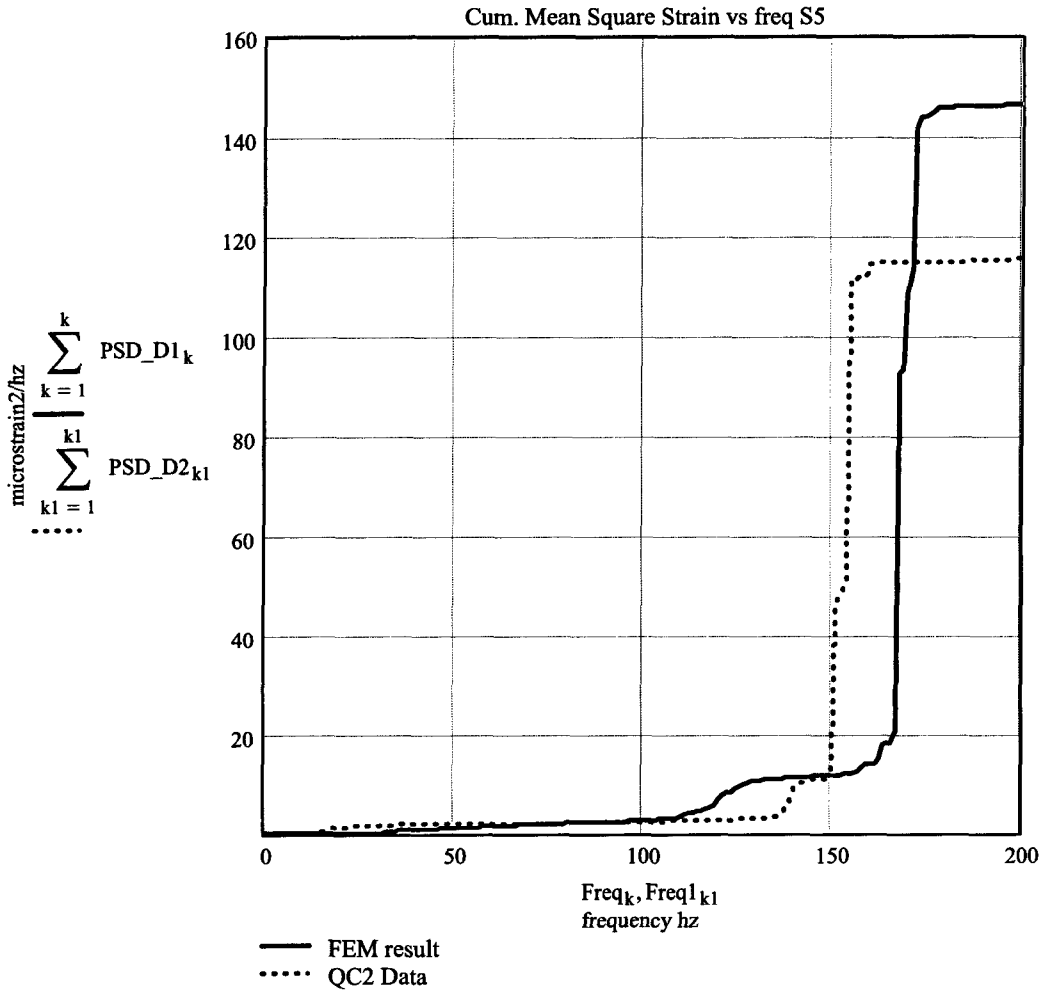

Figure 8 Cumulative Mean Sq Strain Comparison S-7 Minus

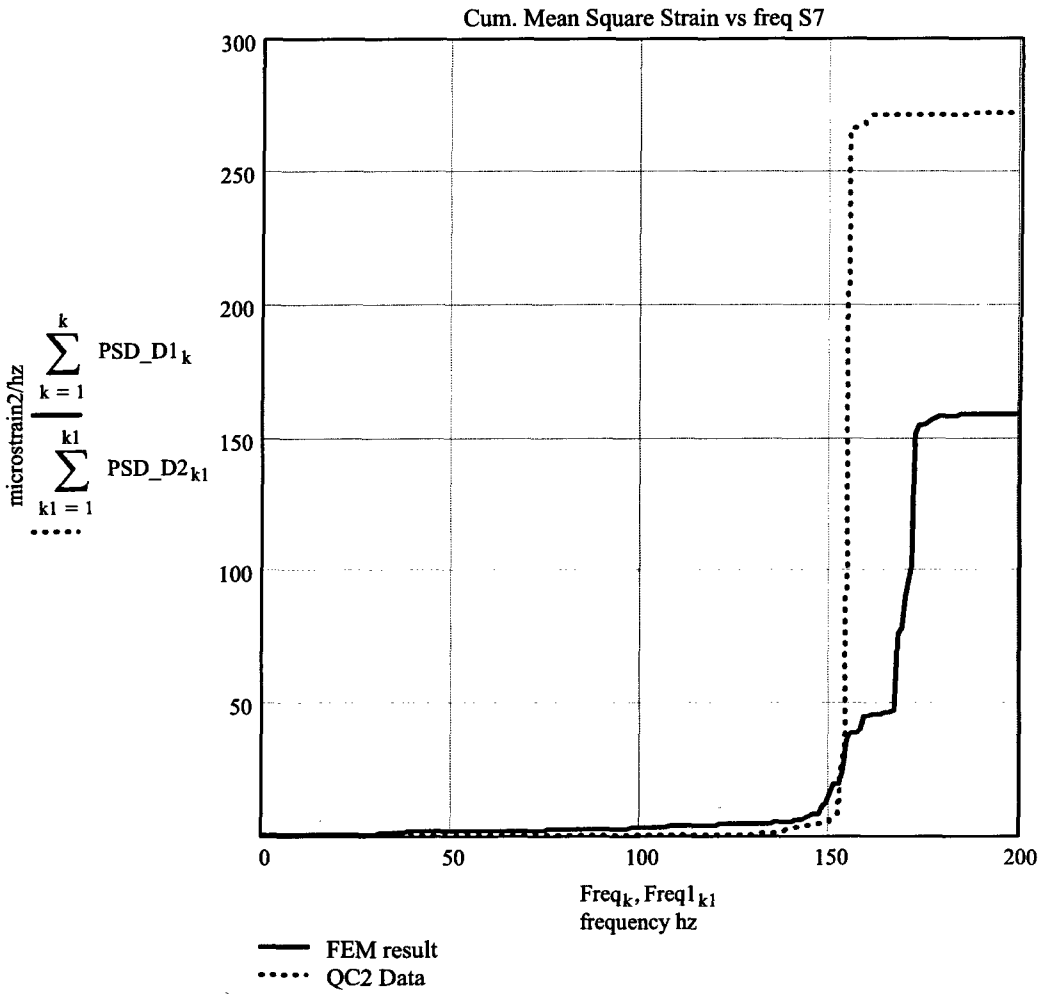

Figure 9 Cumulative Mean Sq Strain Comparison S-8 Minus

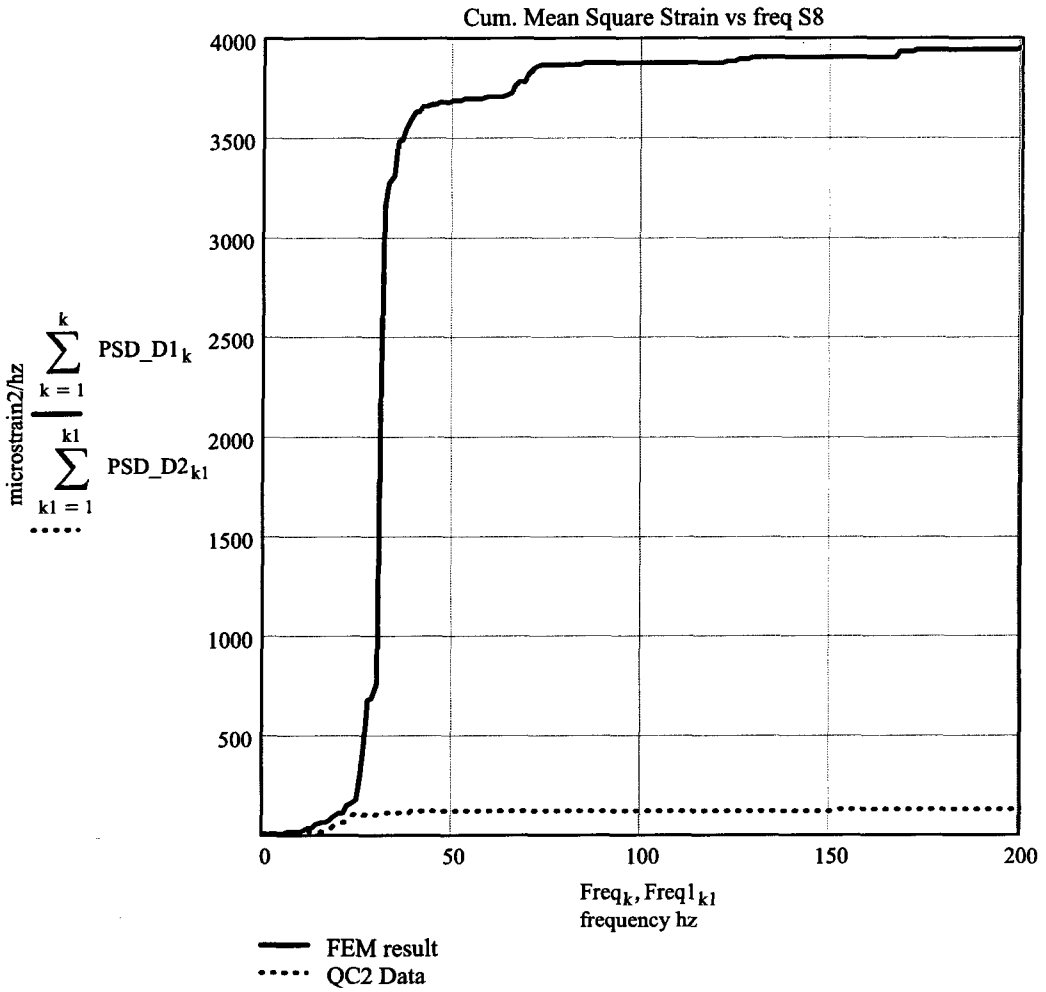

Figure 10 Cumulative Mean Sq Strain Comparison S-9 Minus

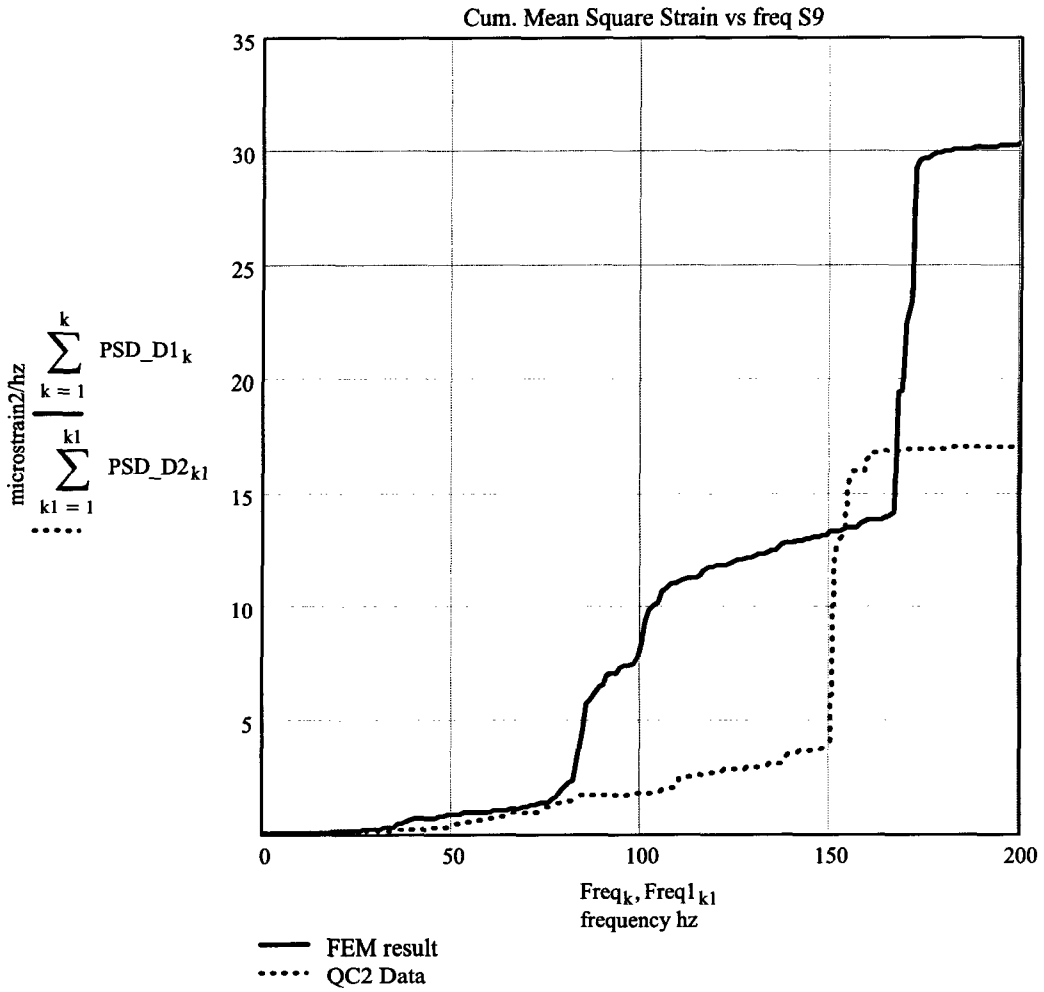

Figure 11 Cumulative Mean Sq Strain Comparison S-1 Plus

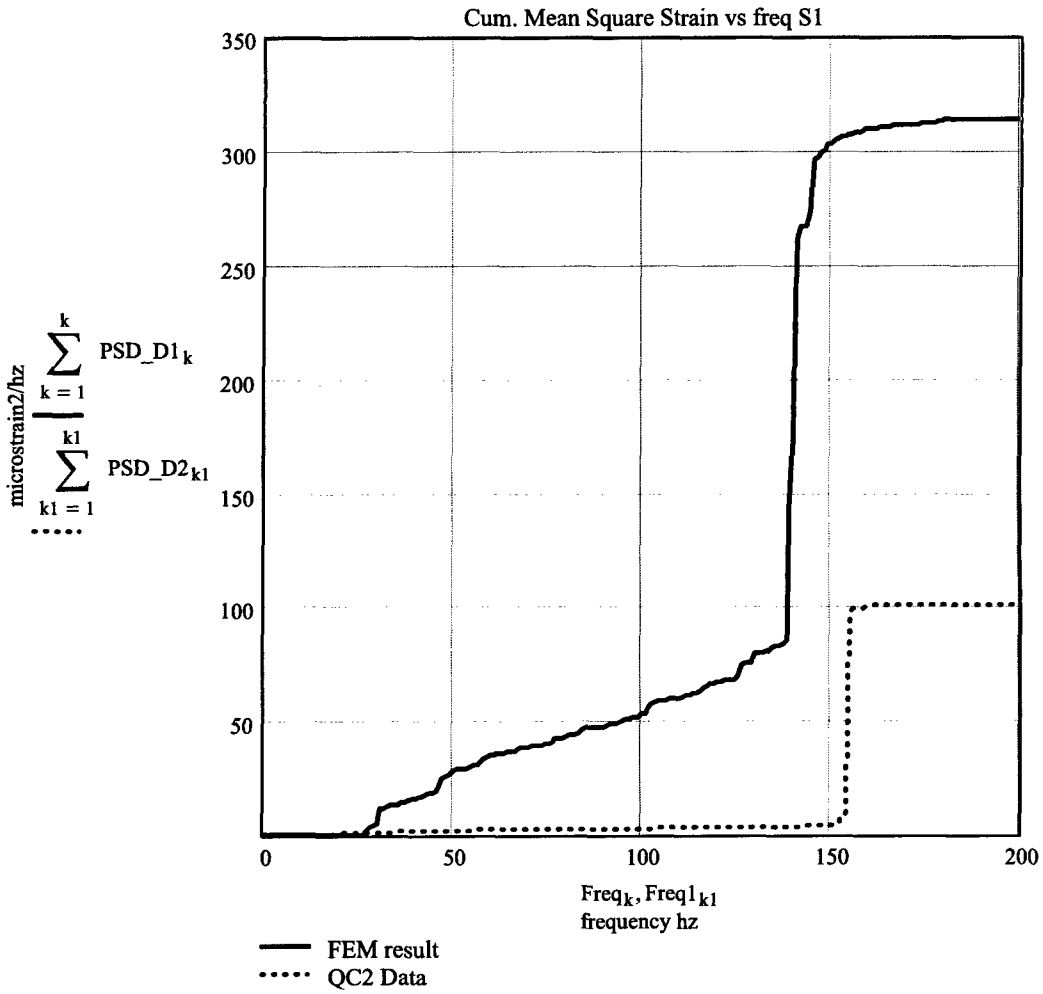

Figure 12 Cumulative Mean Sq Strain Comparison S-5 Plus

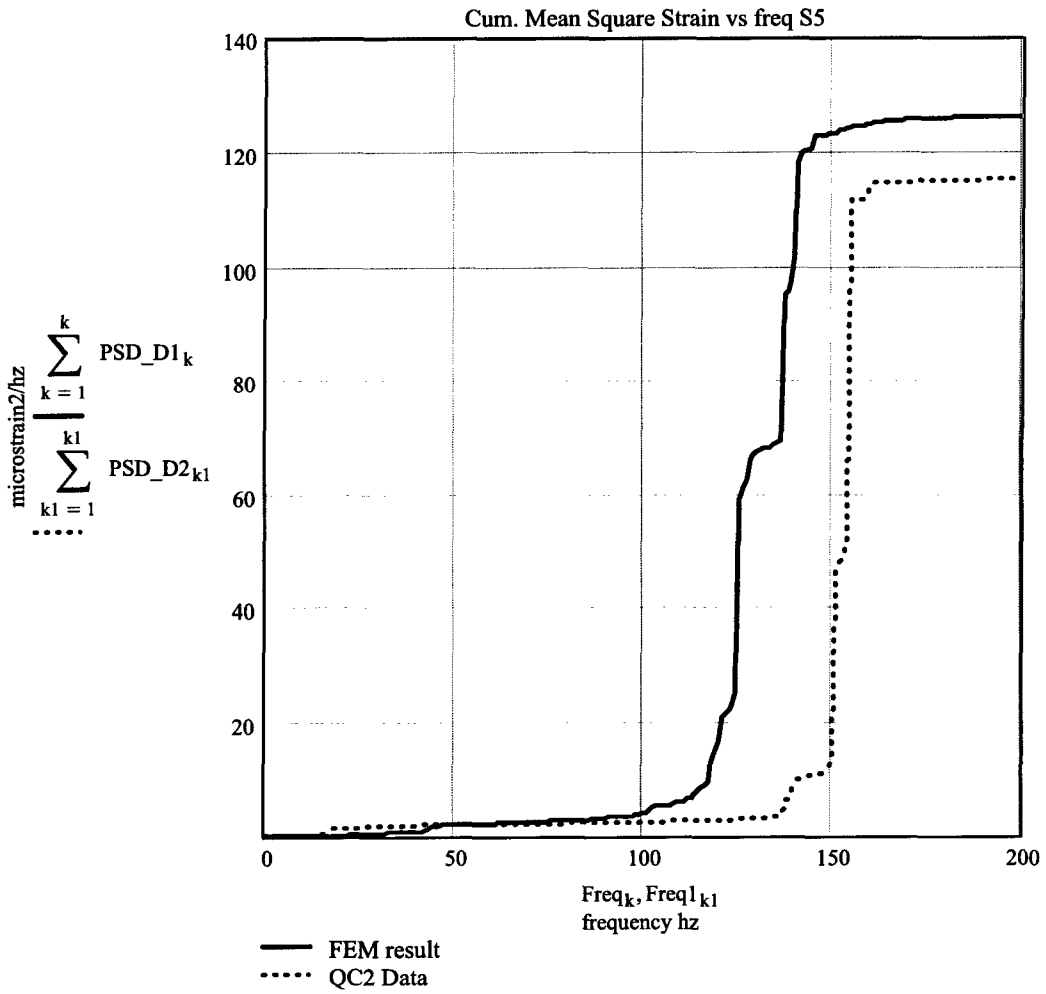

Figure 13 Cumulative Mean Sq Strain Comparison S-7 Plus

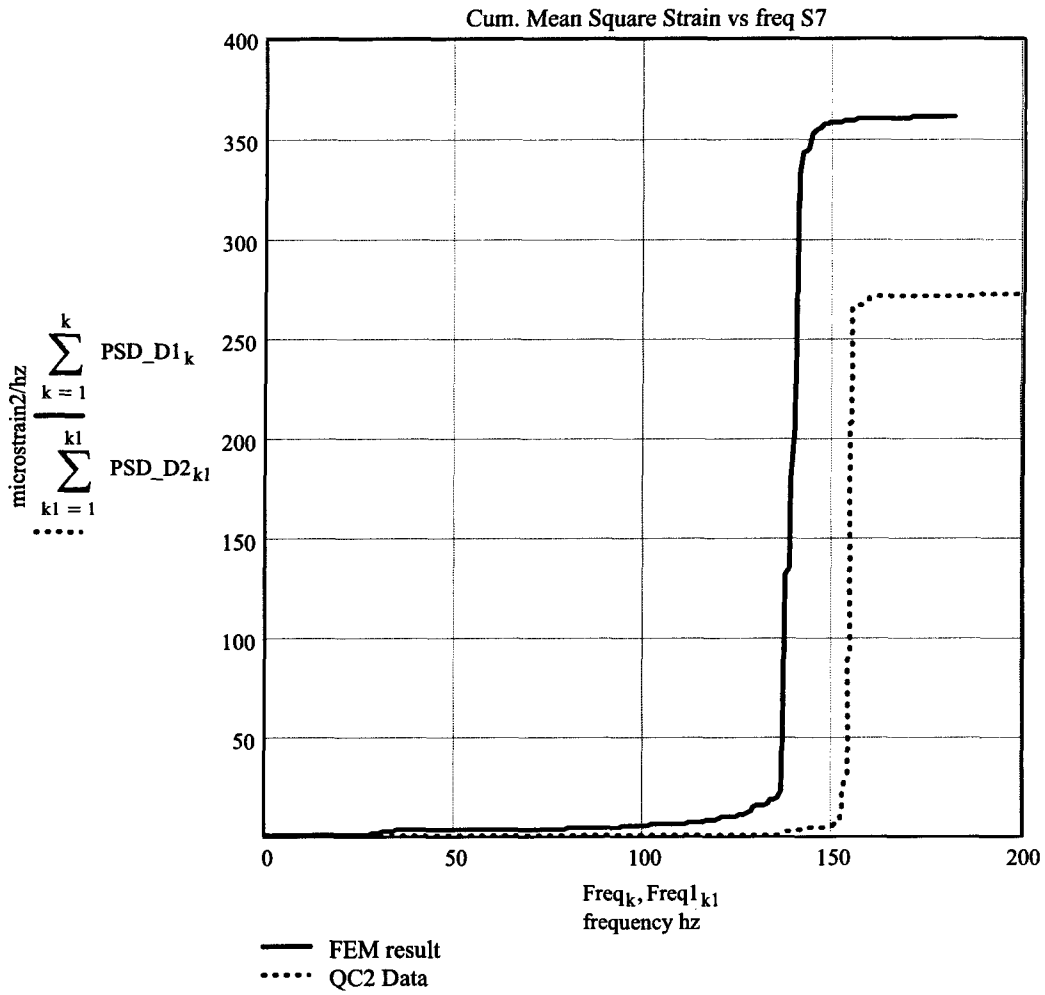

Figure 14 Cumulative Mean Sq Strain Comparison S-8 Plus

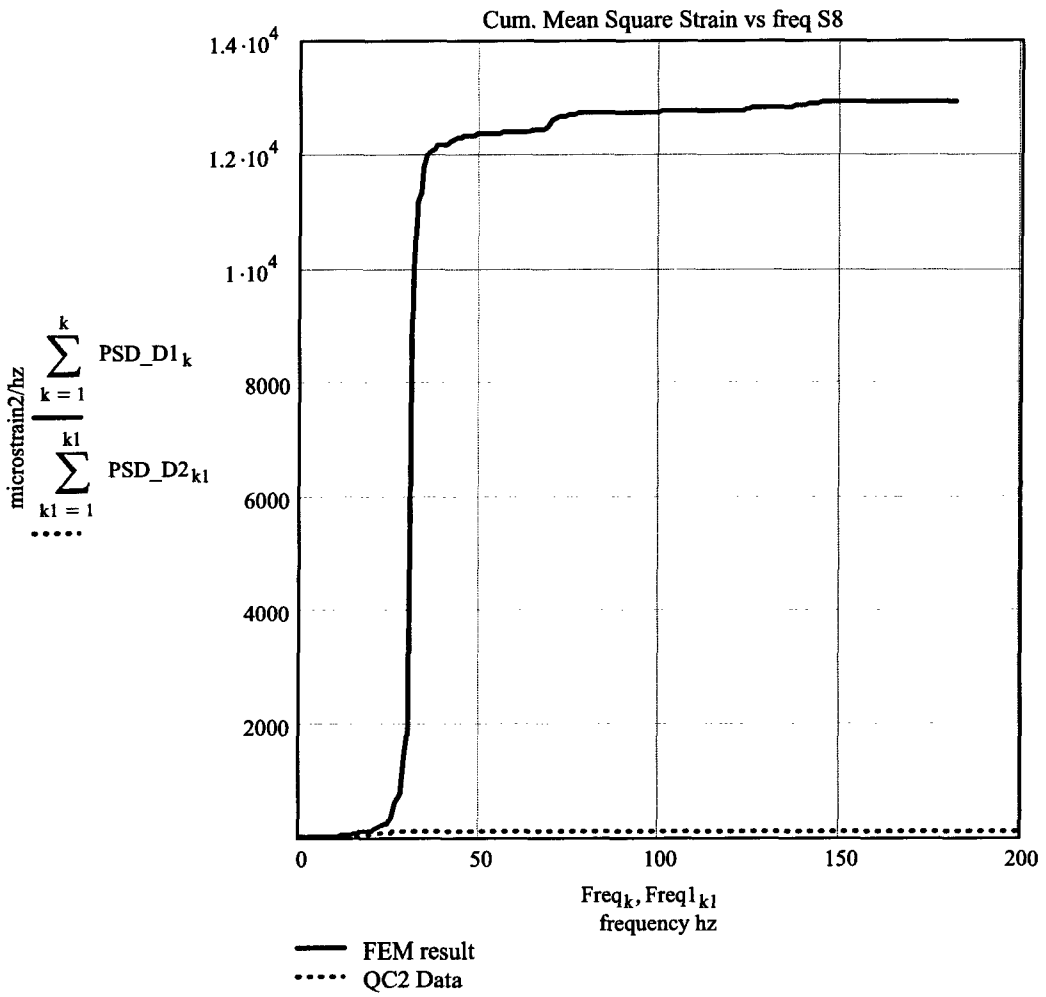

Figure 15 Cumulative Mean Sq Strain Comparison S-9 Plus

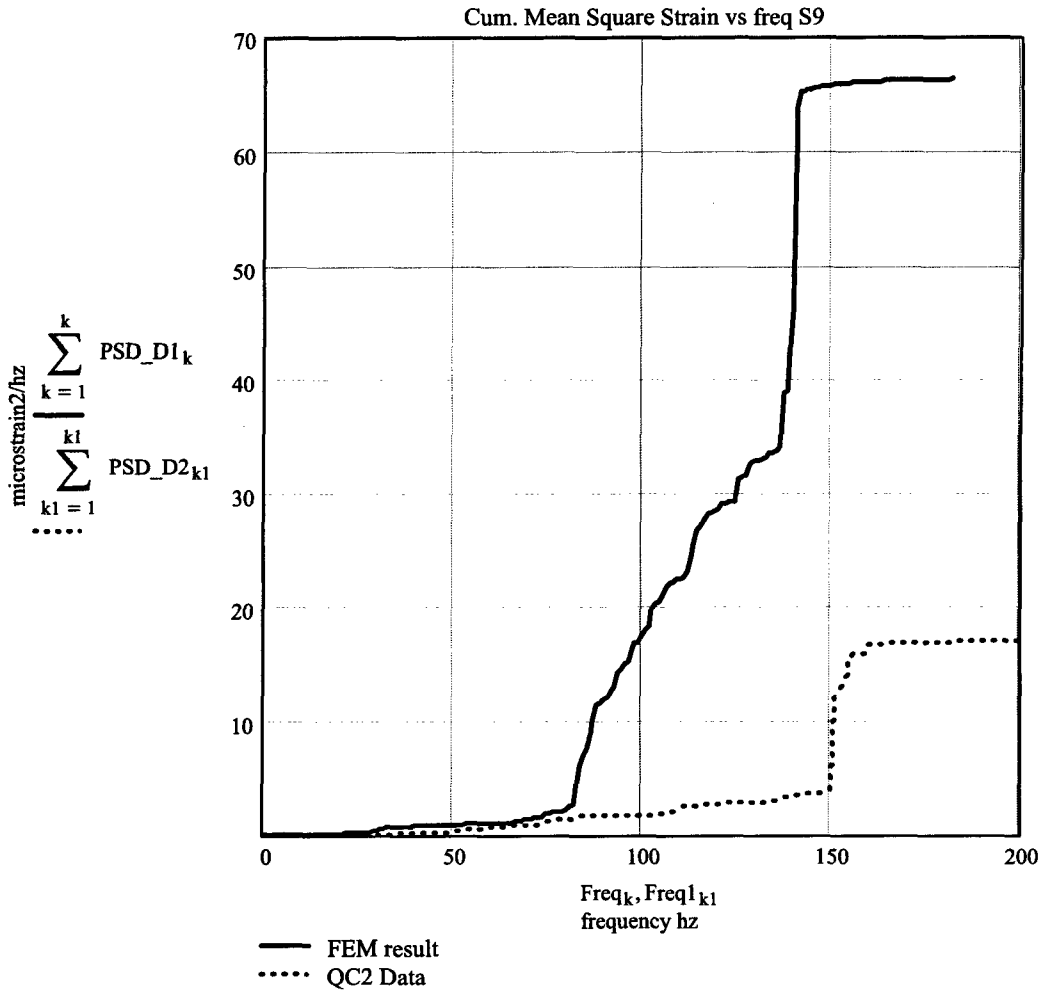

Table 1 Comparison of Nominal Cases

Strain Gage	*Frequency of Main Response (Predict/Measured)*	*Relative change at Main Response Predict/Measured*	*Relative Cumulative Strain*
S-1	151-155/155	3.2	4.25
S-5	150	0.57	0.74
S-7	150-155/155	3.0	3.2
S-8	30/18	80	75
S-9	150/150	1.5	2.1

Table 2 Comparison of –10% Cases

Strain Gage	*Frequency of Main Response (Predict/Measured)*	*Relative change at Main Response Predict/Measured*	*Relative Cumulative Strain*
S-1	165/155	3.4	4.25
S-5	165/150	1.2	1.25
S-7	165/155	0.43	0.6
S-8	31/18	30	29
S-9	165/150	1.3	1.75

Table 3 Comparison of +10% Cases

Strain Gage	*Frequency of Main Response (Predict/Measured)*	*Relative change at Main Response Predict/Measured*	*Relative Cumulative Strain*
S-1	137/155	2.3	3.2
S-5	137/150	0.55	1.12
S-7	137/155	1.2	1.3
S-8	30/18	100	100
S-9	137/150	2.4	3.7

5. Conclusions/Discussion

A comparison of the predicted and measured cumulative mean square strains was performed for QC2 TC41. This comparison was performed to provide insight into the overall performance of the Modified 930 MWe ACM and FEM analysis models. The following conclusions are made based on this work:

1. The analytical models overpredict the structural response at all locations except S-5 for the nominal case and S-7 for the –10% case.

2. When the +/- 10% cases are considered, the analytical models overpredict the structural response at all locations except S-7 for the –10% case.

3. The structural response predicted for the skirt locations is consistent with earlier observations that the loads on the skirt are significantly overpredicted by the Modified 930 MWe ACM.

4. The change in strain occurring at the peak acoustic load frequencies (150-160 Hz) is consistent and conservative relative to the measured results.

Based on the comparisons presented, the Modified 930 MWe ACM coupled with the FEM yields conservative results when compared to plant measured data. The amount of conservatism ranges from 1.25 at the worst location to factors greater than 2 at the other locations on the dryer.

6. References

1. GE-NE-0000-0037-1951-01, Revision 0, "Dryer Vibration Instrumentation Uncertainty," April 2005.
2. "Acoustic Circuit Benchmark, Quad Cities Unit 2 Instrumented Steam Path, 790 MWe and 930 MWe Power Levels," AM-2005-002, Revision 0, June 2005.
3. "Acoustic Circuit Model Validation, Quad Cities Unit 2 Instrumented Steam Path, Final Model Revision 930 MWe Power Level," AM-2005-004, Revision 0, July 2005.
4. "Quad Cities Units 1 and 2 Replacement Steam Dryer Analysis Stress, Dynamic, and Fatigue Analyses for EPU Conditions," DRF GE-NE-0000-0034-3781, Section GE-NE-0000-0039-4902, Revision 0, April 2005.
5. "Quad Cities Unit 1 Replacement Steam Dryer Stress and Fatigue Analysis Based on Measured EPU Conditions," DRF GE-NE-0000-0043-5391, Section GE-NE-0000-0043-9157, Revision 1, August 2005
6. "Quad Cities Unit 2 Replacement Steam Dryer Stress and Fatigue Analysis Based on Measured EPU Conditions," DRF GE-NE-0000-0043-3105-01, Section GE-NE-0000-0043-3119, Revision 0, July 2005.
7. "Strain Gauge Time History Data from QC2A FEA Runs," letter GE-ENG-DRY-136, Richard Bodily to Al Bontjes, data 10/15/2005.

Appendix A- Dryer Sensor Locations

234C6821 REV 2

REVISIONS

1	APR 18 2005 RMCN06047	RJA
2	APR 22 2005 RMCN06057	RJA

✳ ACCELEROMETERS MOUNTED IN OPPOSITE DIRECTION DUE TO ACCESS AND SAFETY.

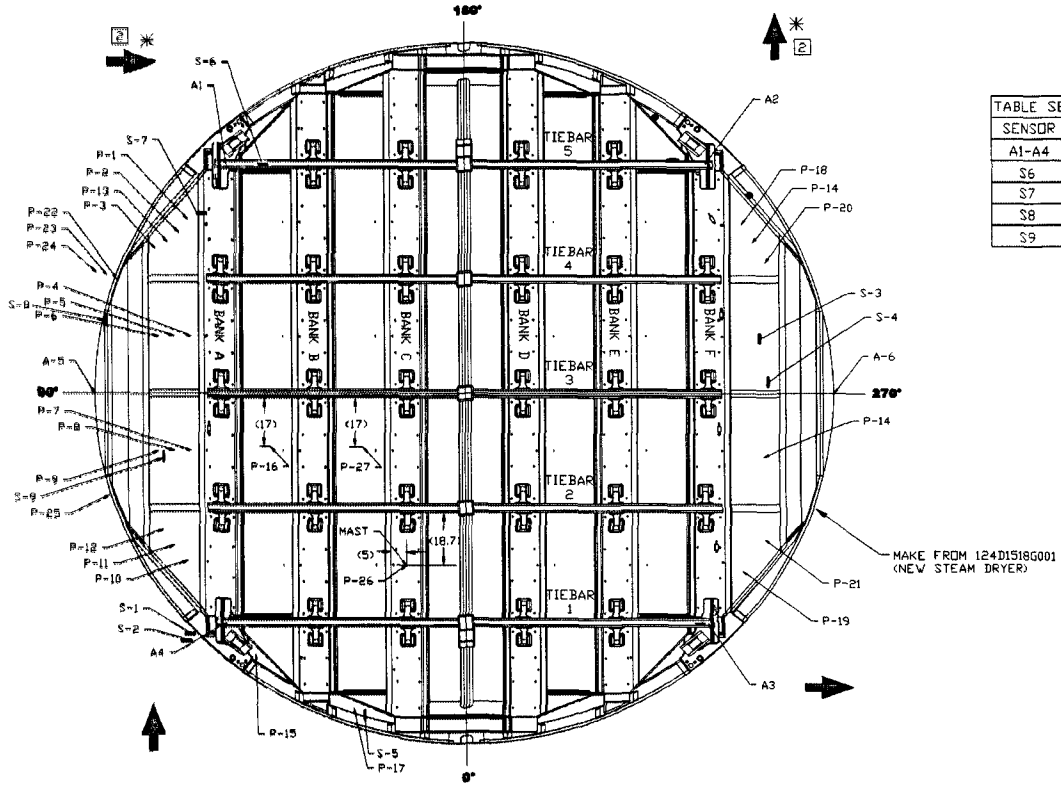

TABLE SENSOR MOUNTING	
SENSOR	MOUNT DETAIL
A1-A4	J
S6	H
S7	H
S8	J
S9	G

DRYER SENSOR LOCATIONS - TOP VIEW

Nuclear Energy

	DAY	MO	YR	DWG NO.	REV.
DRAWN DH CHAN	28	01	01	234C6821	2
CHECKED NA				FEB 28 2005 SH 2 OF 3	

1 AC-234C6821SH2

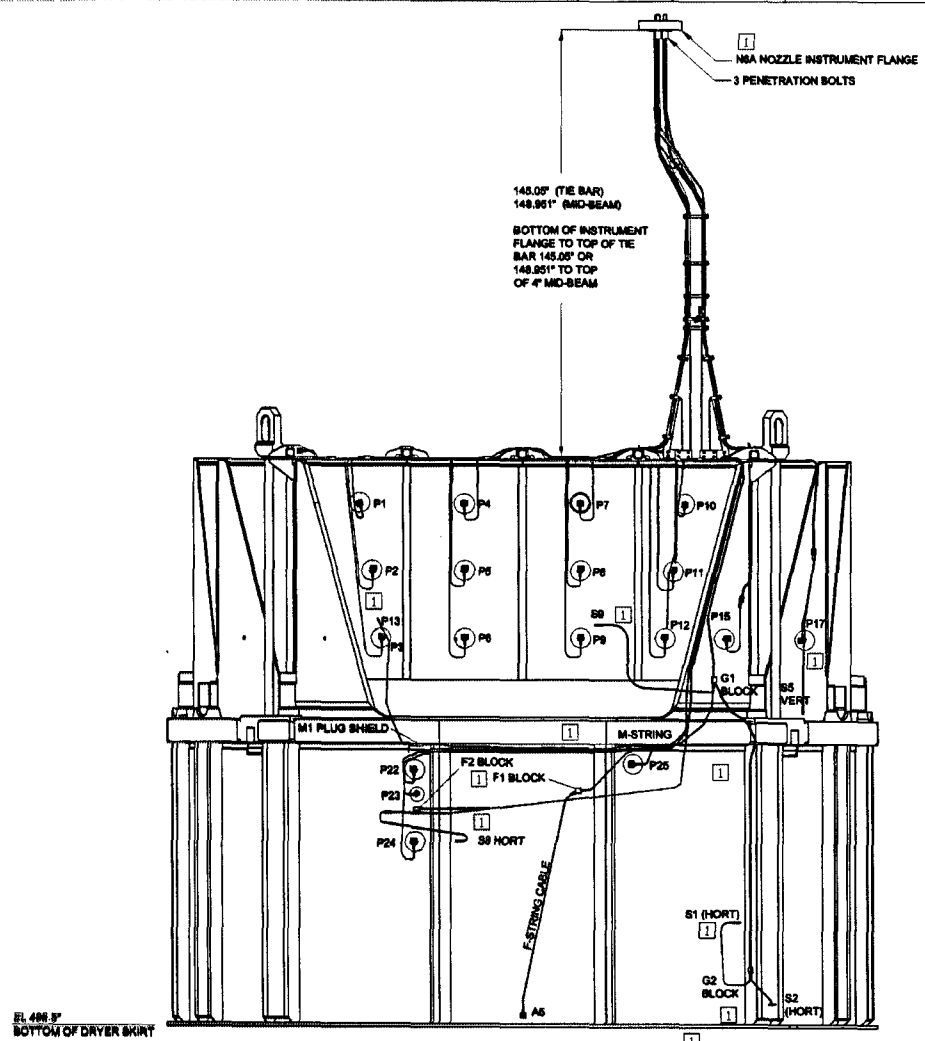

TABLE SENSOR MOUNTING		
SENSOR	MOUNT DETAIL	
P1	B	
P2	B	
P3, P13	D	
P4-P12	B	
P15	B (BOTTOM)	
P17	C (TOP)	
P22	B OR A	
P23	E (INTERNAL)	
P24	B, C, OR A	
P25	B	
S1	G (HORT)	1
S2	G (HORT)	
S8, S9	F (HORT)	1
A5	J (HORT)	

DRYER SENSOR LOCATIONS - 90° FACE

SCALE 1 / 20

234C6821	5			
REVISIONS				
1	APR 18 2005 RMCN06047	RJA		

Nuclear Energy	DAY	MO	YR	DWG NO 234C6821 REV 1
DRAWN DH CHAN	28	01	01	
CHECKED NA				FEB 28 2005 SH 5 OF 6

1 AC-234C6821SH5

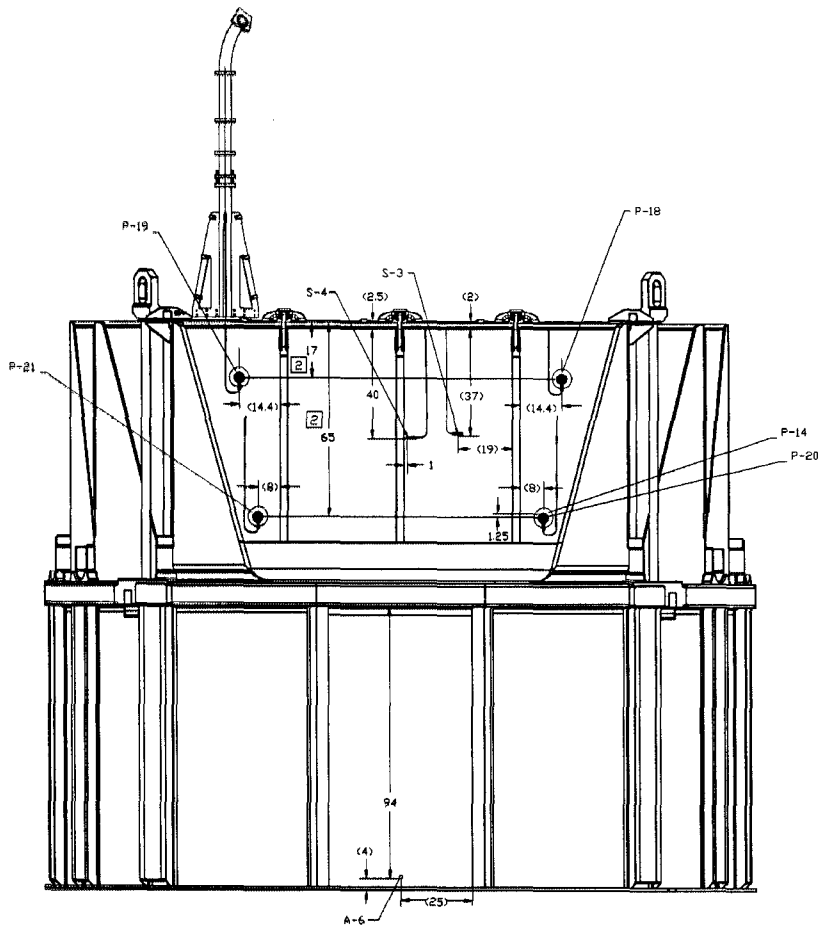

270° FACE (LOOKING TOWARDS CENTER)

DRYER SENSOR LOCATIONS - 270° FACE

TABLE SENSOR MOUNTING	
SENSOR	MOUNT DETAIL
S-3	F (HORT)
S-4	F (HORT)
P18	B
P19	B
P20, P14	D
P21	B
A6	J (HORT)

Nuclear Energy	DAY	MO	YR	DWG NO. 234C6821	REV. 2
DRAWN DH CHAN	28	01	01		
CHECKED NA				FEB 28 2005 SH NO. 6	CONT ON 7

1 AC-234C6821SH6

234C6821 SH NO. 6

REVISIONS

1	APR 18 2005 RMCN06047	RJA
2	APR 22 2005 RMCN06057	RJA

Enclosure 4

C.D.I. Technical Note No. 05-37, "Blind Evaluation Of Continuum Dynamics, Inc. Steam Dryer Load Methodology Against Quad Cities Unit 2 In-Plant Data at 2831 MWt," Revision 2

C.D.I. Technical Note No. 05-37

Blind Evaluation Of Continuum Dynamics, Inc. Steam Dryer Load Methodology Against Quad Cities Unit 2 In-Plant Data At 2831 MWt

Revision 2

Prepared by

Continuum Dynamics, Inc.
34 Lexington Avenue
Ewing, NJ 08618

Prepared under Purchase Order No. 00403055 for

Exelon Generation LLC
4300 Winfield Road
Warrenville, IL 60555

Approved by

Alan Bilanin

Alan J. Bilanin

November 2005

Summary

Measured in-plant strain gage data, recorded in the four main steam lines of Quad Cities Unit 2 (QC2) at 2831 MWt (TC39), were collected at two positions upstream of the ERV standpipes on each of the main steam lines and were used to drive an acoustic circuit model of the QC2 steam dome and steam lines. The strain gage data were first converted to pressures, and were then used to extract acoustic sources in the system. Once these sources were obtained, the model was validated by predicting the pressure time histories at 26 locations on the instrumented dryer, where operational pressure sensors were positioned. These predictions were produced blind, i.e., without knowledge of the pressure sensor data, then subsequently compared against the pressure sensor data. Modeling parameters were NOT changed from the parameters developed previously for the "Modified Evaluation" [1], which resulted from examining data taken at 2885 MWt (TC41).

This effort provides Exelon with an additional evaluation of the modified acoustic circuit model parameters that come directly from evaluating against measured dryer data, and compares model predictions using the "Modified Evaluation" parameters at both 2493 MWt (TC32) and 2885 MWt.

It is argued by comparing measured and predicted strains (done by others) that the model parameters for the "Modified Evaluation" provide nearly a factor of two conservatism in predicted stress and therefore the "Modified Evaluation" parameters are appropriate for use in dryer stress evaluations.

Introduction

In Spring 2005 Exelon installed new steam dryers into QC2 and Quad Cities Unit 1. This replacement design, developed by General Electric, sought to improve dryer performance and overcome structural inadequacies identified on the original dryers, which had been in place for the last 30 years. As a means for validating the acoustic circuit analysis, the QC2 dryer was instrumented with pressure sensors at 27 locations. These pressure data formed the set of data to be first predicted (blind evaluation) and then corrected (modified evaluation) utilizing only data measured on the main steam lines. Initial data investigation was undertaken at 790 MWe (2493 MWt), just short of Original Licensed Thermal Power (OLTP) conditions, and at 930 MWe (2885 MWt), near Extended Power Uprate (EPU) conditions. This effort is discussed in [1].

Following release of [1], Exelon requested that Continuum Dynamics, Inc. (C.D.I.) conduct an additional blind evaluation, subsequently providing the strain gage data at 912 MWe (2831 MWt).

Model Predictions and Comparisons

Model evaluation consisted of utilizing the Acoustic Circuit Model with the "Modified Evaluation" model parameters, developed in [1], with additional strain gage data taken at eight main steam line locations by Exelon. The process involved the following chronological steps:

1. The main steam line strain gage data for 2831 MWe (TC39) were provided by Exelon personnel to C.D.I.

2. A blind prediction of the pressures at the locations of the 26 pressure sensors on the dryer was made with the model parameters determined from the "Modified Evaluation" discussed in [1]. This prediction covered approximately 65 seconds of data collection after trigger (a trigger signal matches the strain gage data with the pressure sensor data).

3. The predictions at the 26 operational pressure sensors on the steam dryer were provided to Exelon personnel.

4. Then, Exelon personnel provided the pressure sensor data collected on the steam dryer to C.D.I.

5. A comparison was made between the predictions and the data at the operational pressure sensors, and margin was evaluated.

Table 1 summarizes the blind evaluation for all operational sensors. Figures 1 to 26 compare the Power Spectral Density (PSD) of the blind predictions with the data at 912 MWe, while Figure 27 compares the pressure range (the maximum pressure minus the minimum pressure) and RMS values at the pressure sensors.

Figure 28 compares the ratio of predicted pressure to data for the three power levels examined by C.D.I. Here the parameters examined are the pressure range and the RMS of the pressure. Note that if this ratio is greater than 1.0, the prediction is conservative. This result indicates that the Acoustic Circuit Model using "Modified Evaluation" parameters is somewhat more conservative at lower power levels.

Figure 29 is constructed by summing the predicted range over all 21 transducer locations on the external surfaces of the dryer and dividing this sum by the sum of the measured range of the 21 transducers. Similarly, this same ratio is computed for RMS values. Since it is believed that it is the peak pressure on the dryer that correlates with peak stresses, the range curve is indicative of the global conservatism in the loading methodology. The average peak load is conservative at low power in excess of 30% and is conservative at highest power by about 5%. Note that transducers P13, P14, P16, P23 and P27 are not included in this summation, as they are not located on external dryer surfaces.

Discussion and Conclusions

Figure 29 shows that the acoustic circuit model predictions of RMS are nonconservative by about 5% between 900 MWe and 930 MWe (specifically at 912 MWe). Figure 28 shows that, similar to previous predictions at 930 MWe [1], pressure sensor signals are underpredicted by the model. This is a consequence of a model prediction acceptance criterion that required only that model predictions be within 90% of the data for pressure sensors P3, P12, P20, and P21. This criteria was probably motivated by the fact that error analysis of pressure transducers

located on the dryer are anticipated to measure fluctuating pressures with a high bias of up to 10% as a consequence of installation hardware [2].

In an effort to further improve model predictions with data, additional sensitivity analyses were undertaken. The goal of these analyses was to raise the level of pressures predicted for transducers located above the elevation of the main steam line inlets, without raising the level on transducers located below that elevation. It was determined that decreasing the damping in the steam dome accomplished this objective. It is believed that previous benchmarking and model tuning settled on a steam dome damping value that was too large, and it is now believed that most of the damping of acoustic waves occurs inside the steam dryer, where surface areas are large and the steam froth interface absorbs most of the radiated acoustic energy.

Specifically, Exelon asked C.D.I. to refine the model parameters driving the acoustic circuit prediction, in the 145 – 165 Hz range. These parameters include: (1) the absorption at the steam froth interface beneath the dryer; (2) the absorption at the steam water interface between the skirt and the steam dome; (3) the damping in the steam dome; and (4) the damping in the main steam lines. C.D.I. has been able to bound nearly all of the signals measured at the 26 operational pressure sensors by a modest reduction of damping in the steam dome and a comparable increase in damping in the main steam line [3]. Further refinements are expected to result in a conservative simulation of all of the pressure sensors.

The acoustic circuit model load predictions are then input into a finite element structural model of the dryer. A fair question to ask is, do the predictions shown in this report translate into a conservative prediction of strain from the finite element model? Exelon has shown independently [4] that the finite element model predictions are conservative by as much as a factor of two in prediction of strain on the dryer, when compared with data. These comparisons [4] show cumulative strain predicted by the finite element model with strain gage data. Thus, the Modified Evaluation acoustic circuit model provides loads that result in conservative predictions of stress (up to a factor of two) and suggests that building additional margin into the acoustic circuit model is not justified.

Reference

1. Continuum Dynamics, Inc. 2005. Evaluation of Continuum Dynamics, Inc. Steam Dryer Load Methodology. C.D.I. Report No. 05-10.

2. Exelon Corporation. 2005. An Assessment of the Uncertainty in the Application of the Modified 930 MWe Acoustic Circuit Model Predictions For the Replacement Quad Cities Units 1 and 2 Steam Dryers. Document No. AM-2005-0012.

3. Continuum Dynamics, Inc. 2005. Improved Methodology to Predict Full Scale Steam Dryer Loads from In-Plant Measurements. C.D.I. Report No. 05-23 (to be issued).

4. Exelon Corporation. 2005. A Comparison of the Cumulative Mean Square Strain in the Application of the Modified 930 MWe Acoustic Circuit Model and FEA to the QC2 TC41 In-Vessel Test Condition. Document No. AM-2005-0010.

Table 1. Comparison between the 912 MWe data and modified evaluation predictions. The data have been filtered to include the frequencies from 0 Hz to 200 Hz only.

Pressure Sensor Number	Data Minimum (psid)	Predicted Minimum (psid)	Data Maximum (psid)	Predicted Maximum (psid)	Data RMS (psid)	Predicted RMS (psid)
P1	-1.263	-1.070	1.114	1.127	0.362	0.311
P2	-1.226	-0.813	1.187	0.893	0.410	0.205
P3	-1.684	-1.845	1.589	1.853	0.468	0.509
P4	-0.829	-0.581	0.815	0.649	0.250	0.160
P5	-0.930	-0.640	0.900	0.629	0.274	0.153
P6	-1.175	-1.407	1.232	1.382	0.344	0.361
P7	-0.988	-0.598	0.926	0.618	0.295	0.183
P8	-1.125	-0.694	1.087	0.772	0.345	0.180
P9	-1.275	-1.436	1.272	1.502	0.408	0.425
P10	-0.919	-1.244	0.930	1.132	0.286	0.326
P11	-1.104	-0.736	1.079	0.769	0.335	0.182
P12	-1.608	-1.508	1.640	1.520	0.519	0.479
P13	-0.522	-0.194	0.509	0.257	0.142	0.054
P14	-0.785	-0.240	0.760	0.293	0.247	0.073
P15	-1.410	-1.086	1.447	1.162	0.447	0.267
P16	-0.490	-0.156	0.512	0.163	0.146	0.040
P17	-0.656	-0.815	0.655	0.850	0.192	0.215
P18	-1.041	-1.275	1.060	1.278	0.379	0.435
P19	failed	failed	failed	failed	failed	failed
P20	-1.411	-1.787	1.321	1.842	0.440	0.500
P21	-1.910	-2.476	1.962	2.417	0.776	0.798
P22	-1.272	-2.183	1.154	2.132	0.337	0.544
P23	-0.367	-0.120	0.347	0.133	0.097	0.031
P24	-0.729	-0.971	0.669	0.986	0.182	0.236
P25	-0.977	-1.996	1.000	1.915	0.315	0.561
P26	-0.278	-0.161	0.278	0.180	0.077	0.040
P27	-0.513	-0.124	0.514	0.157	0.188	0.034

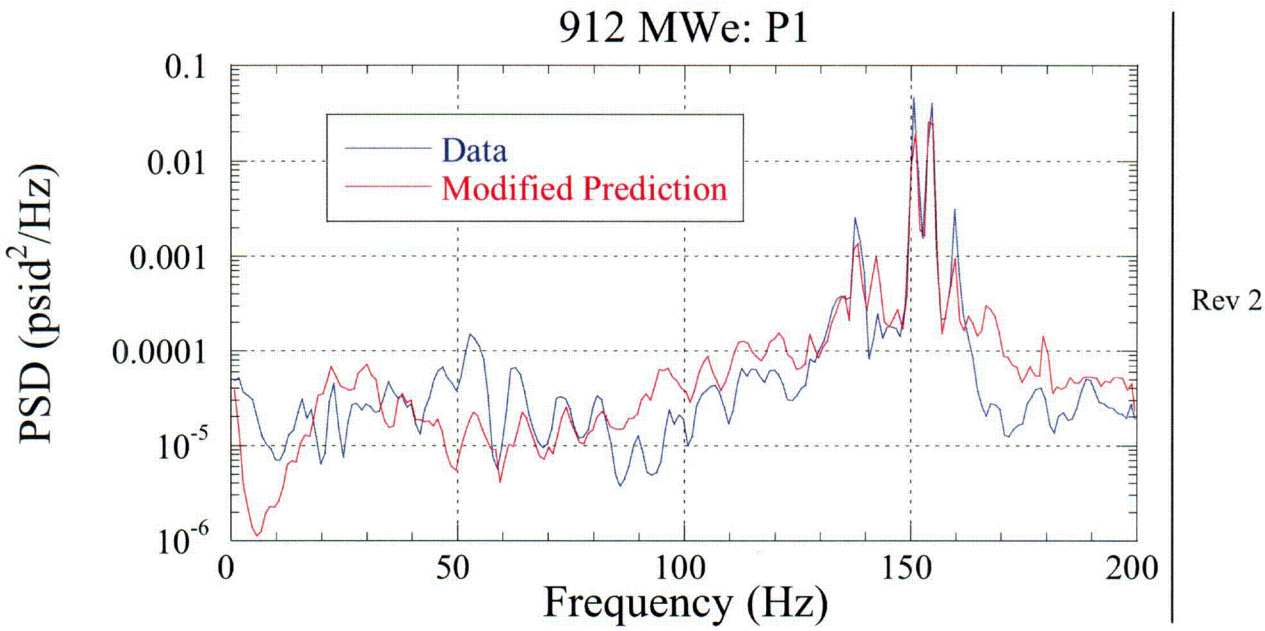

Figure 1. PSD comparison between pressure sensor data (blue curve) and the modified prediction (red curve), for P1.

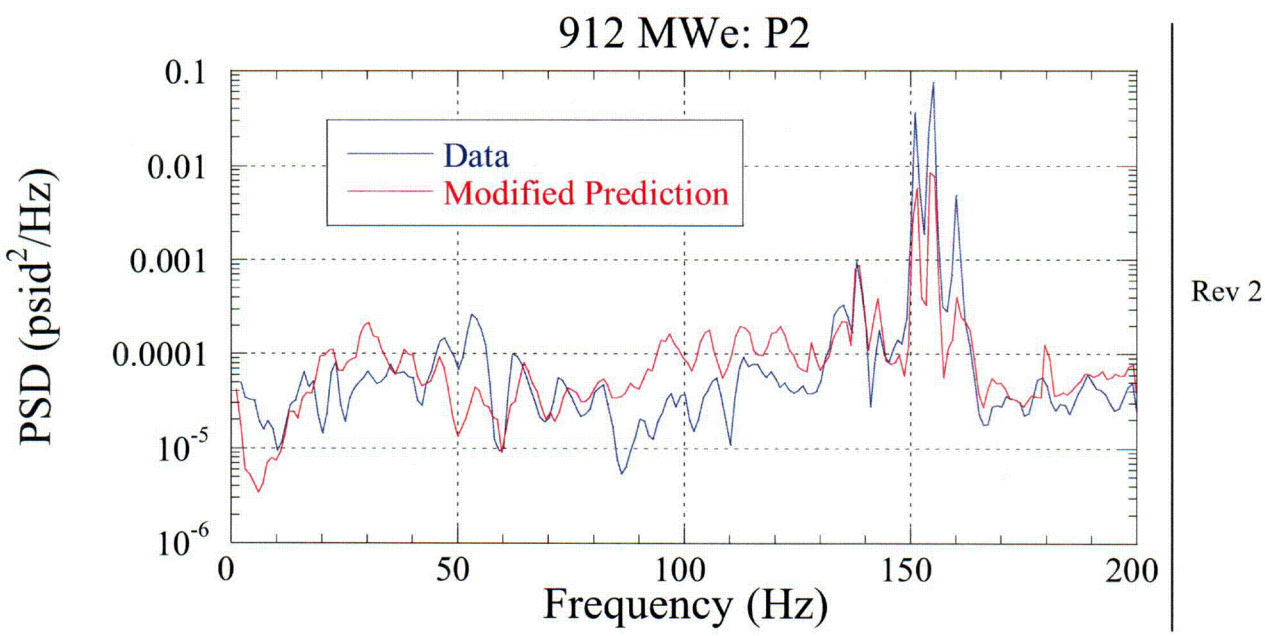

Figure 2. PSD comparison between pressure sensor data (blue curve) and the modified prediction (red curve), for P2.

C01

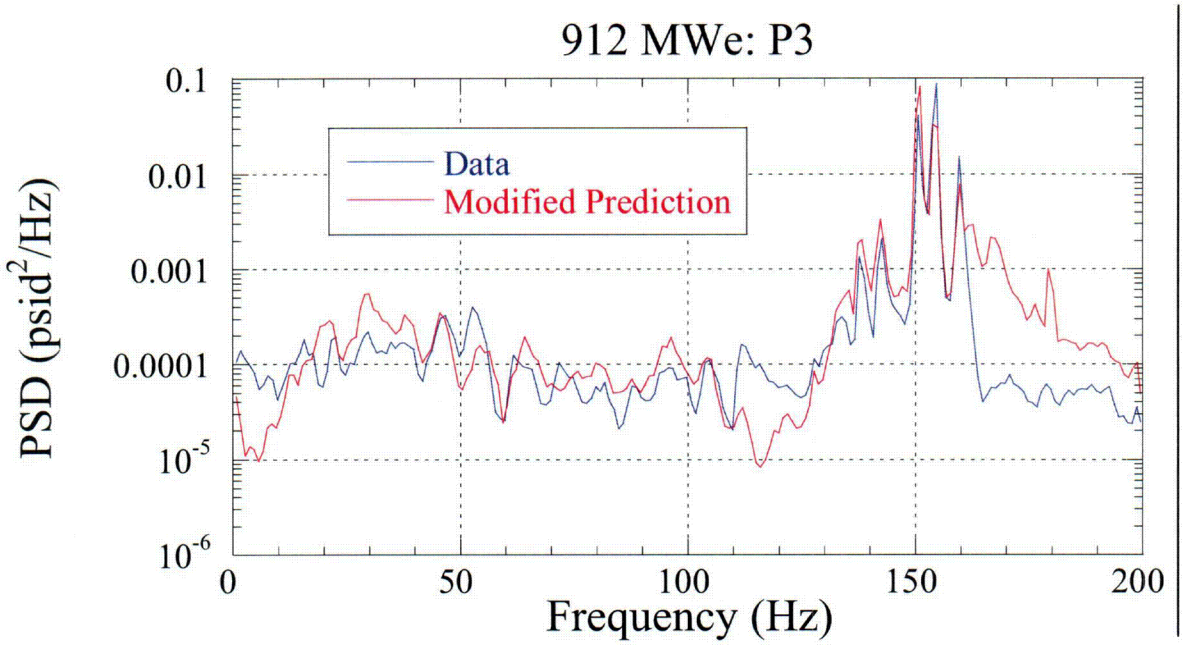

Rev 2

Figure 3. PSD comparison between pressure sensor data (blue curve) and the modified prediction (red curve), for P3.

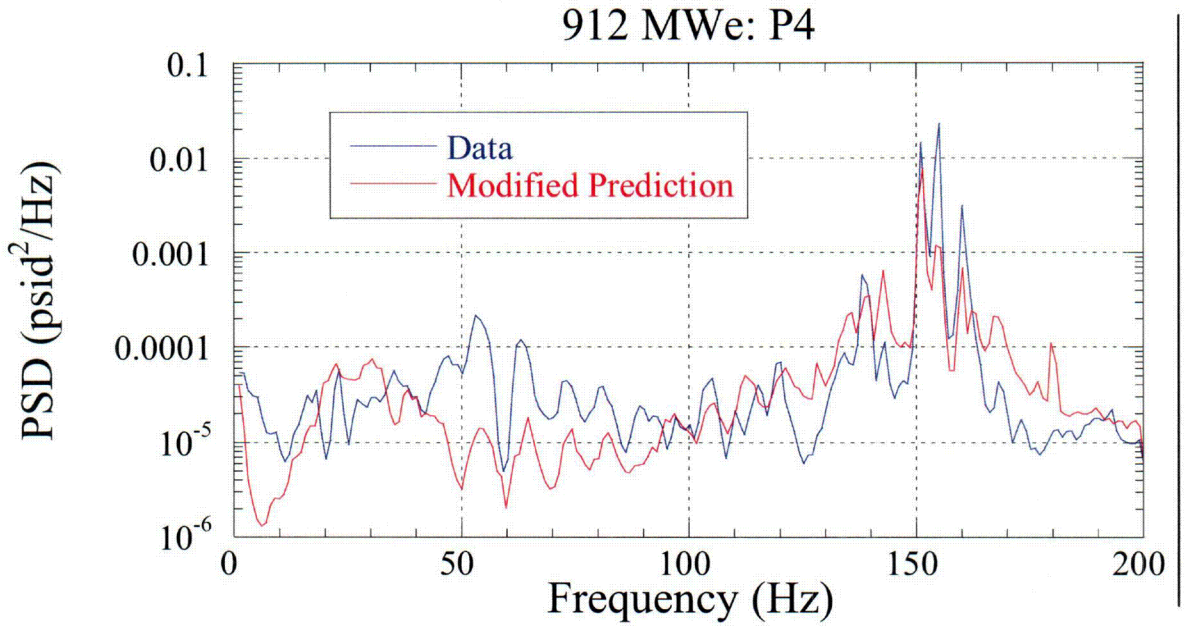

Rev 2

Figure 4. PSD comparison between pressure sensor data (blue curve) and the modified prediction (red curve), for P4.

C02

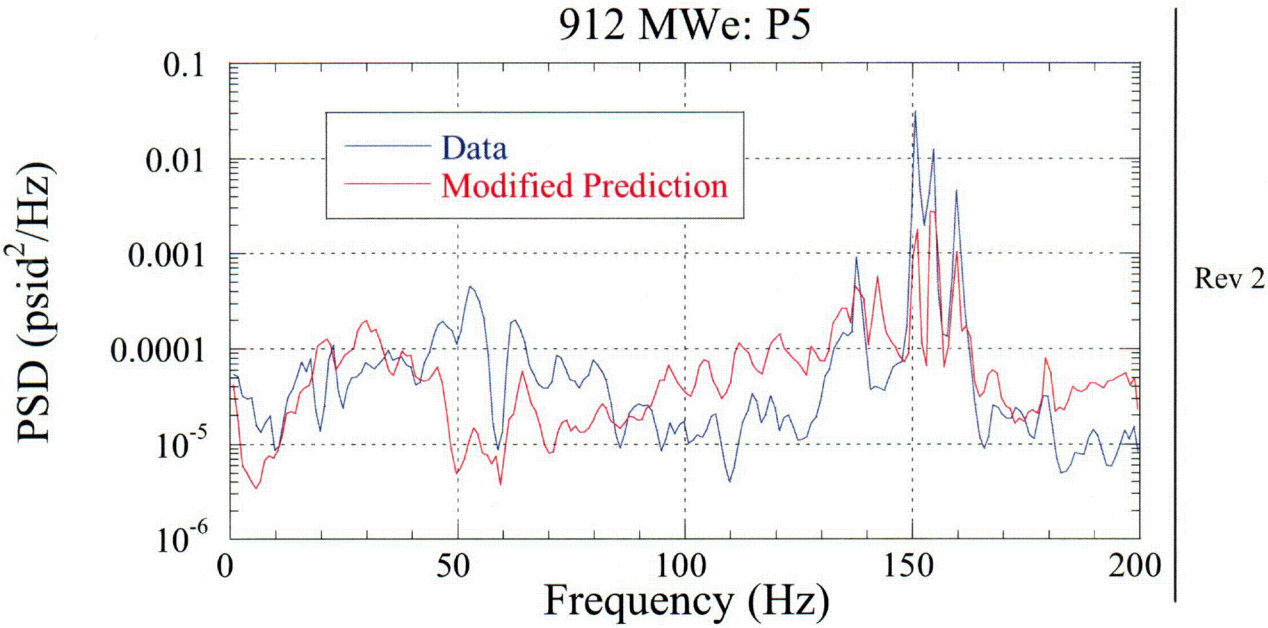

Figure 5. PSD comparison between pressure sensor data (blue curve) and the modified prediction (red curve), for P5.

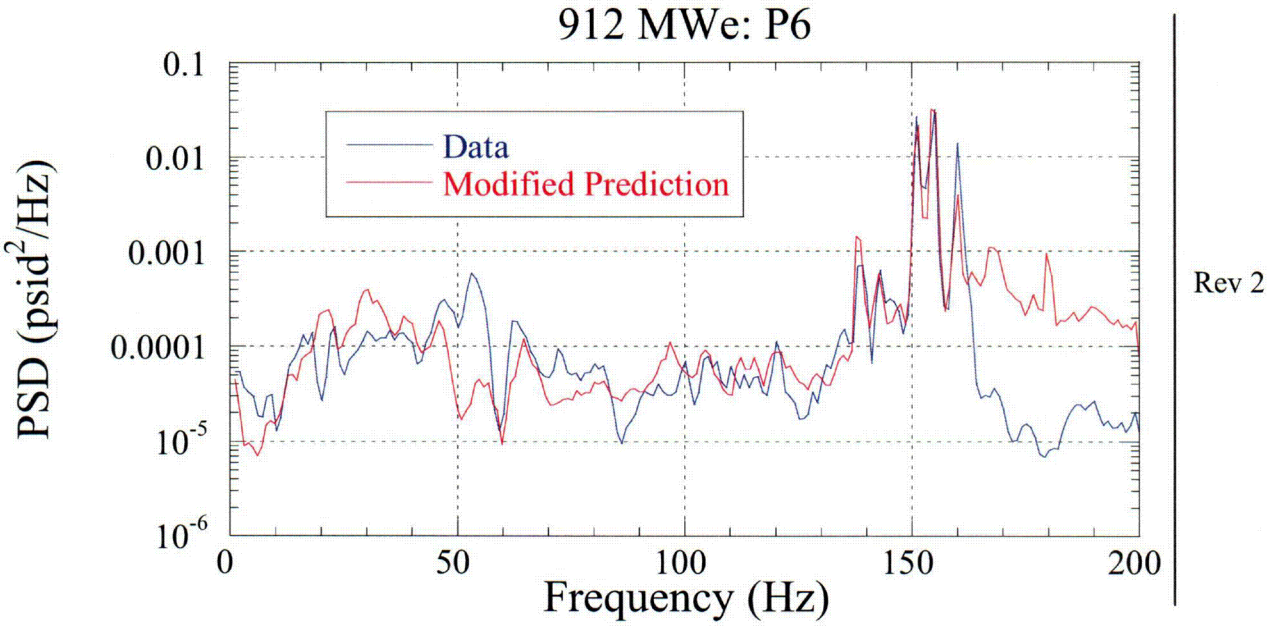

Figure 6. PSD comparison between pressure sensor data (blue curve) and the modified prediction (red curve), for P6.

C03

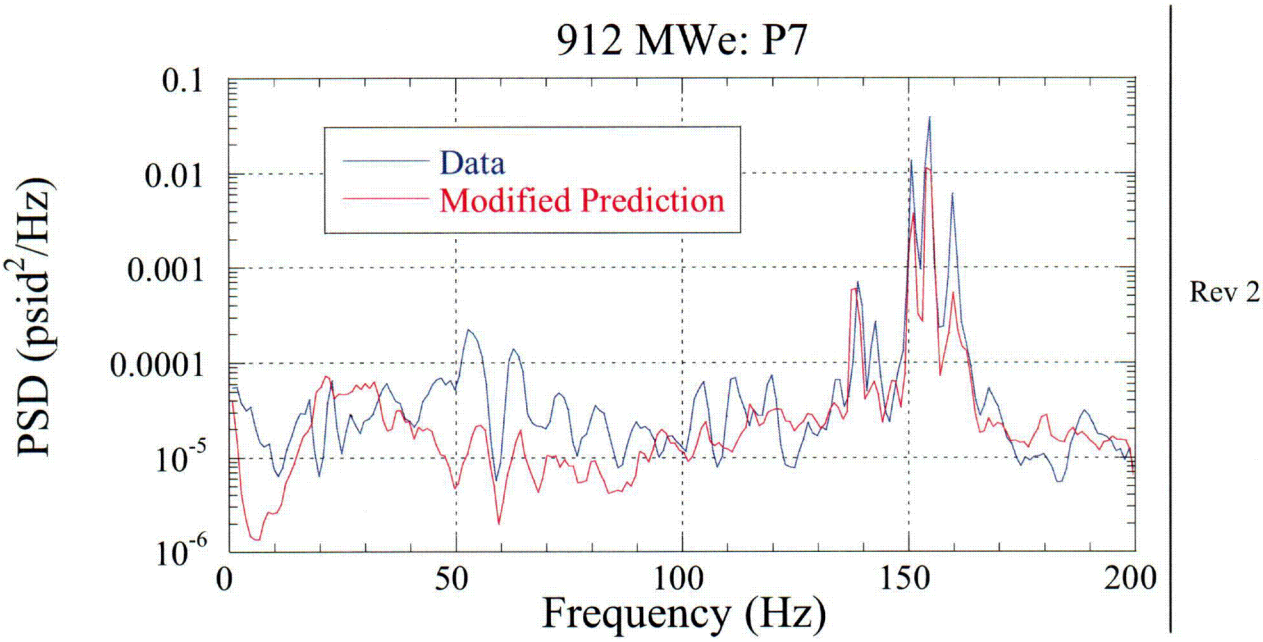

Figure 7. PSD comparison between pressure sensor data (blue curve) and the modified prediction (red curve), for P7.

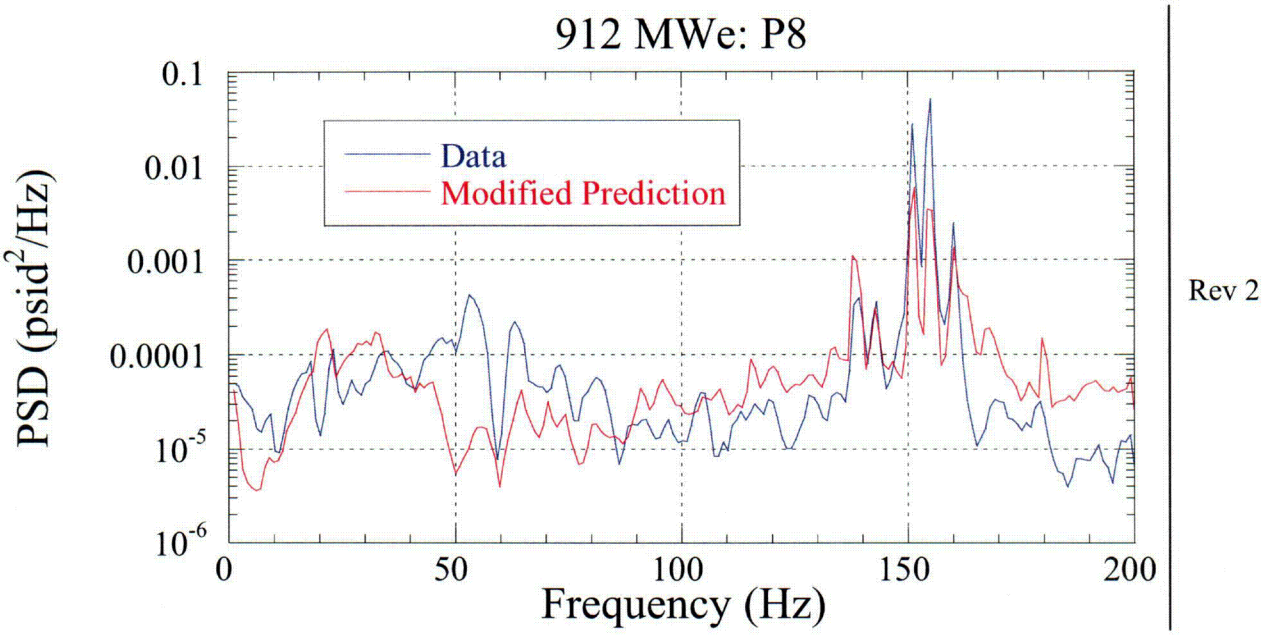

Figure 8. PSD comparison between pressure sensor data (blue curve) and the modified prediction (red curve), for P8.

C04

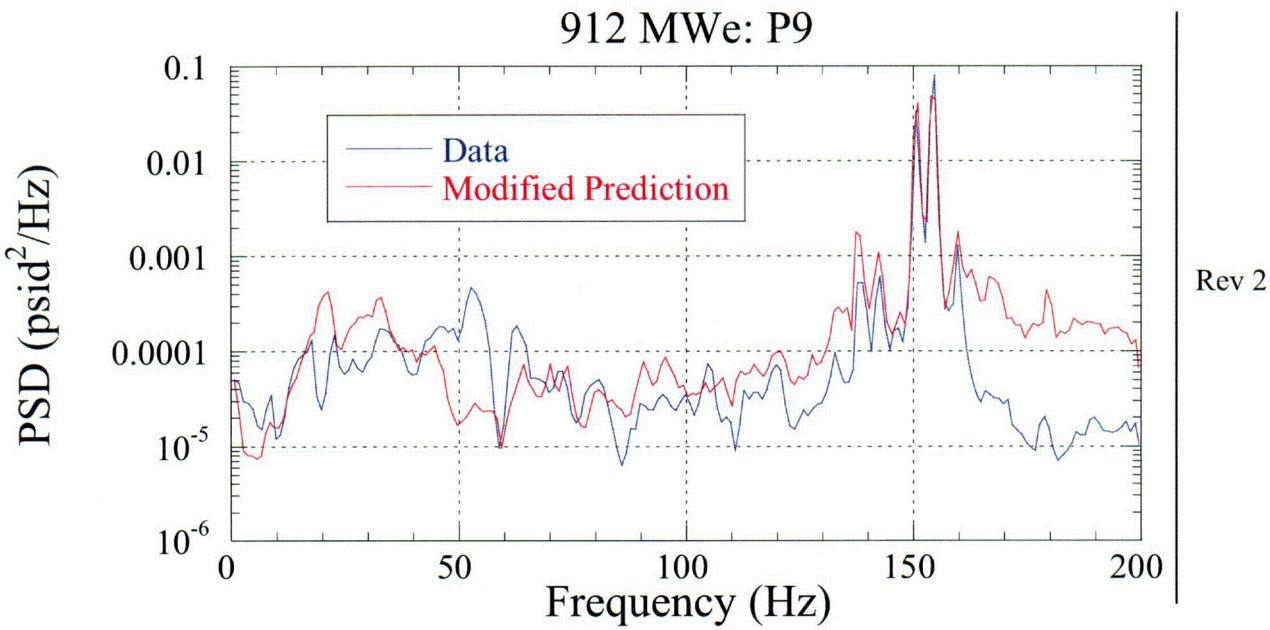

Figure 9. PSD comparison between pressure sensor data (blue curve) and the modified prediction (red curve), for P9.

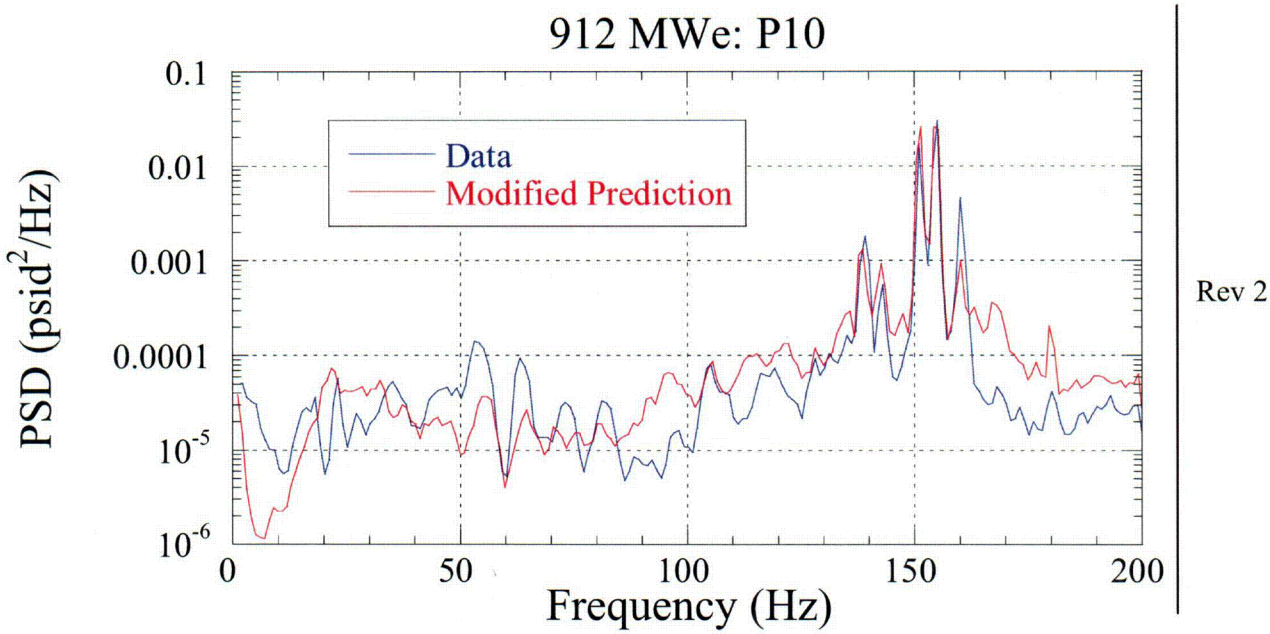

Figure 10. PSD comparison between pressure sensor data (blue curve) and the modified prediction (red curve), for P10.

C05

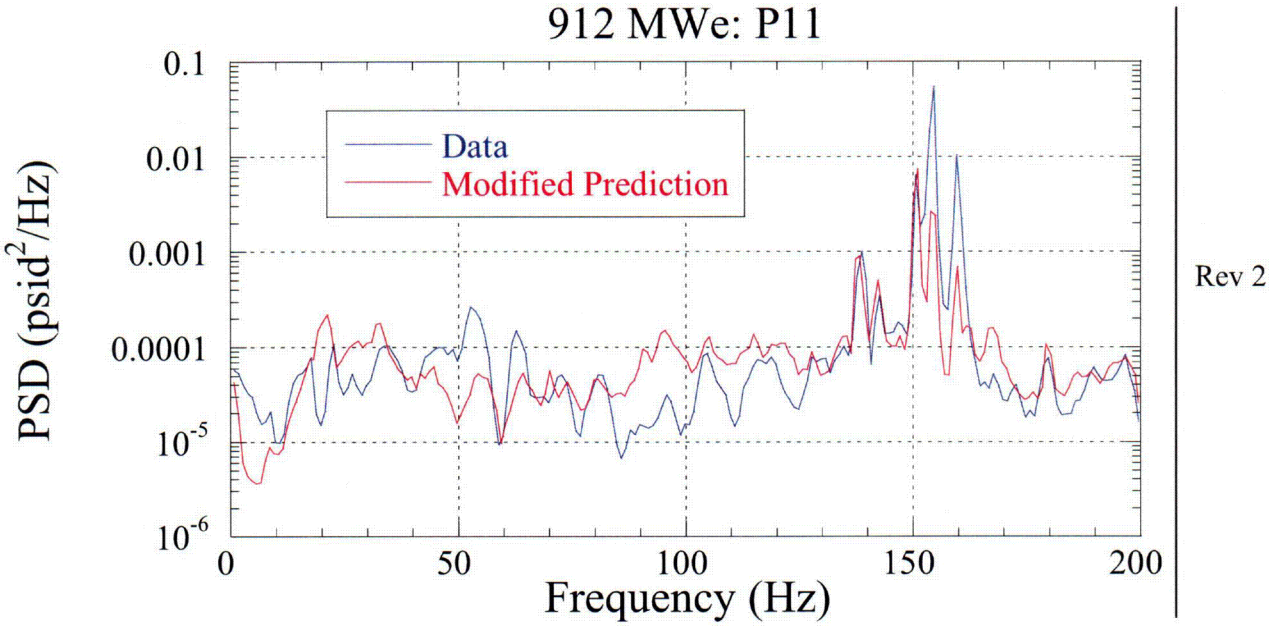

Figure 11. PSD comparison between pressure sensor data (blue curve) and the modified prediction (red curve), for P11.

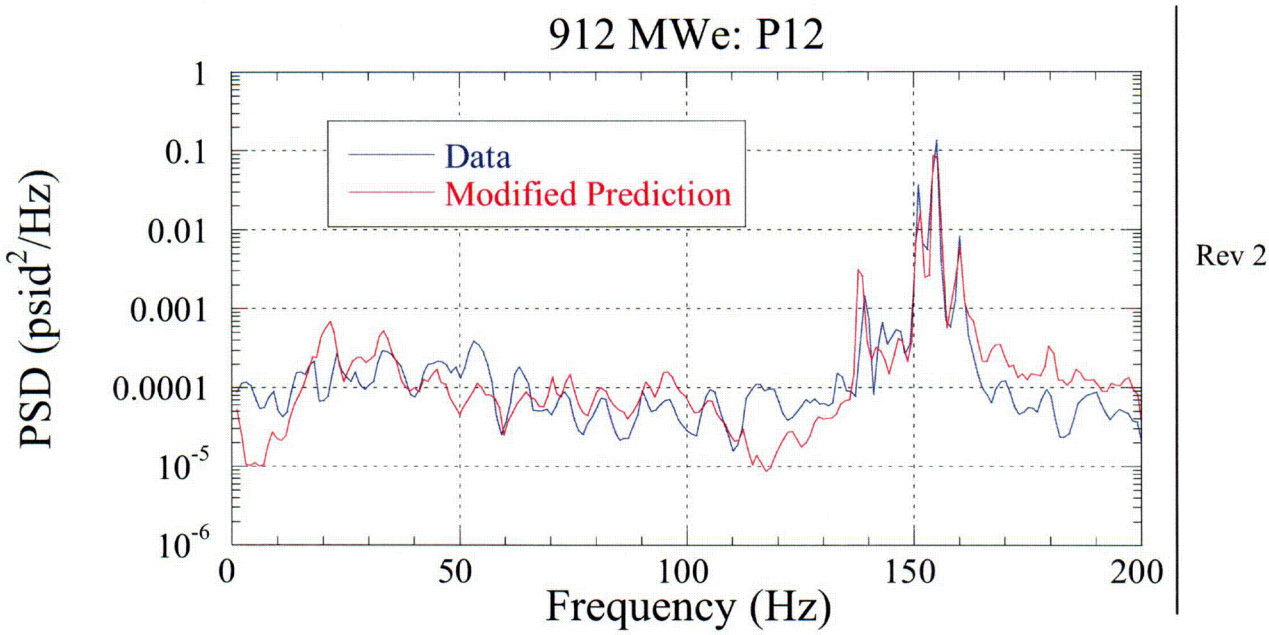

Figure 12. PSD comparison between pressure sensor data (blue curve) and the modified prediction (red curve), for P12.

C06

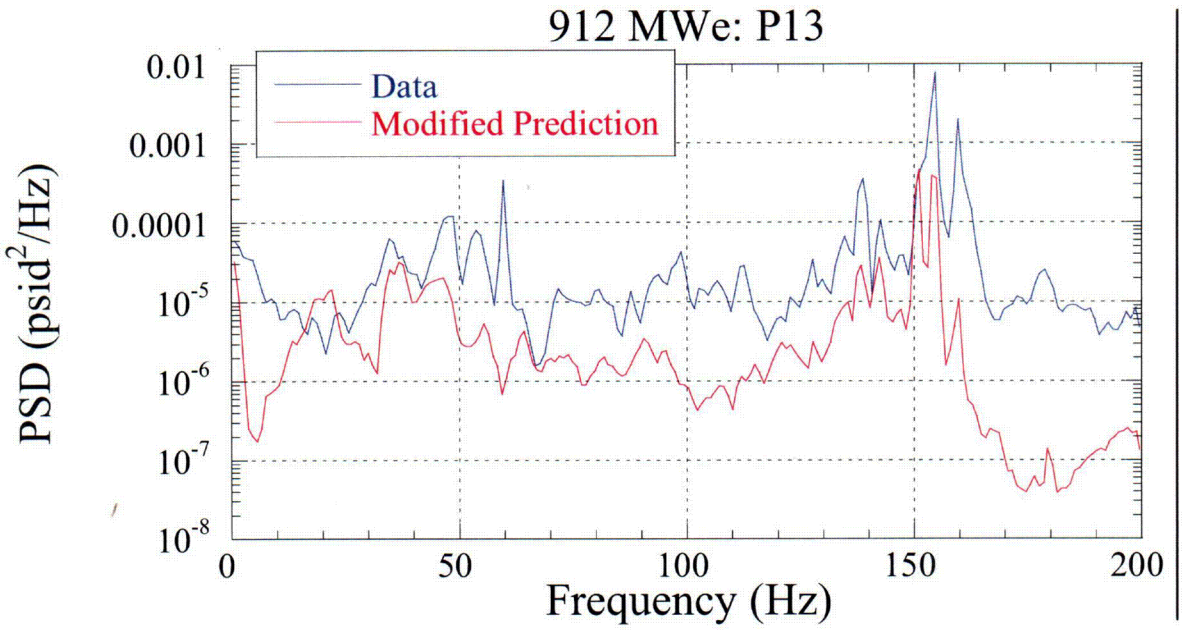

Rev 2

Figure 13. PSD comparison between pressure sensor data (blue curve) and the modified prediction (red curve), for P13 (which is inside the dryer).

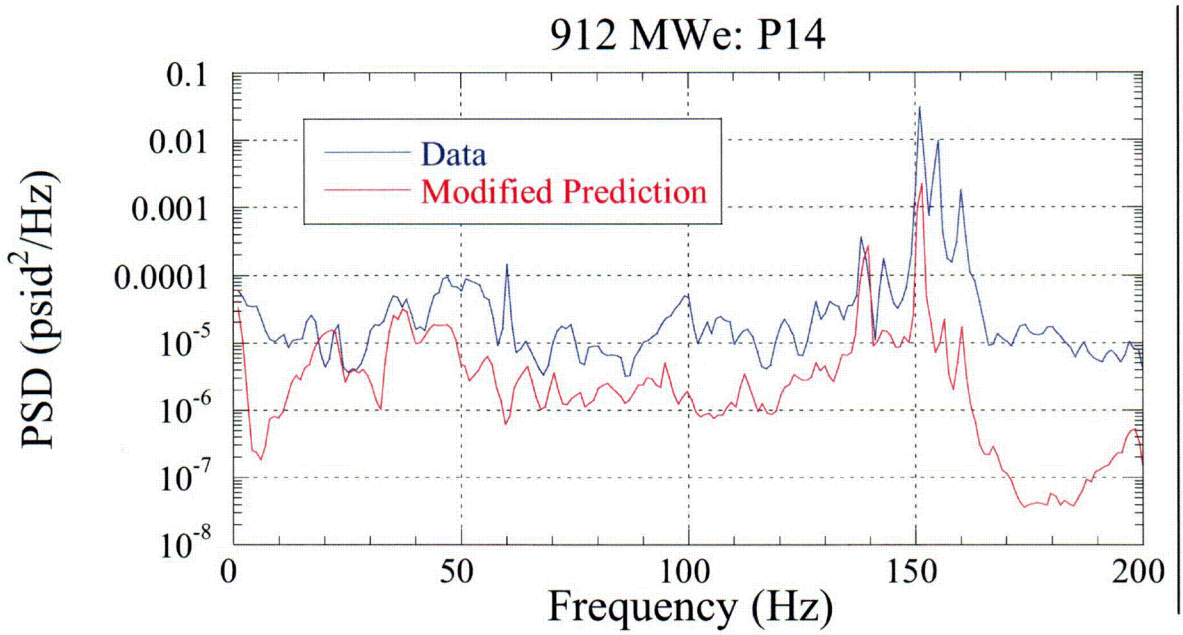

Rev 2

Figure 14. PSD comparison between pressure sensor data (blue curve) and the modified prediction (red curve), for P14 (which is inside the dryer).

C07

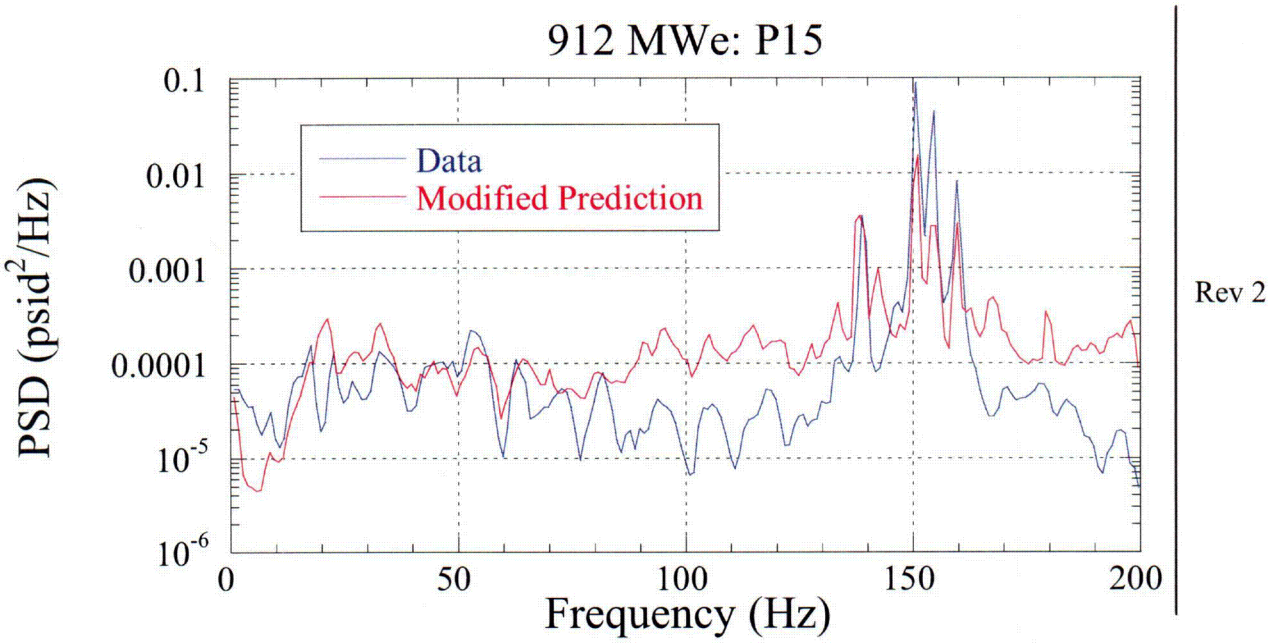

Figure 15. PSD comparison between pressure sensor data (blue curve) and the modified prediction (red curve), for P15.

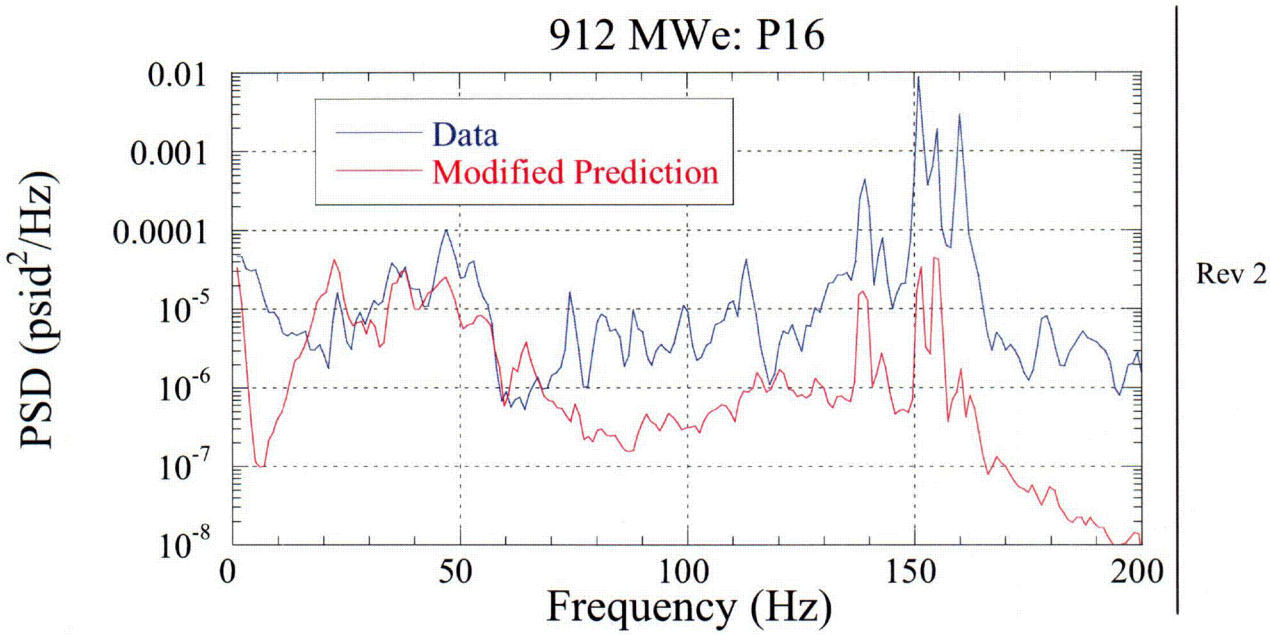

Figure 16. PSD comparison between pressure sensor data (blue curve) and the modified prediction (red curve), for P16 (which is on an inner bank hood).

C08

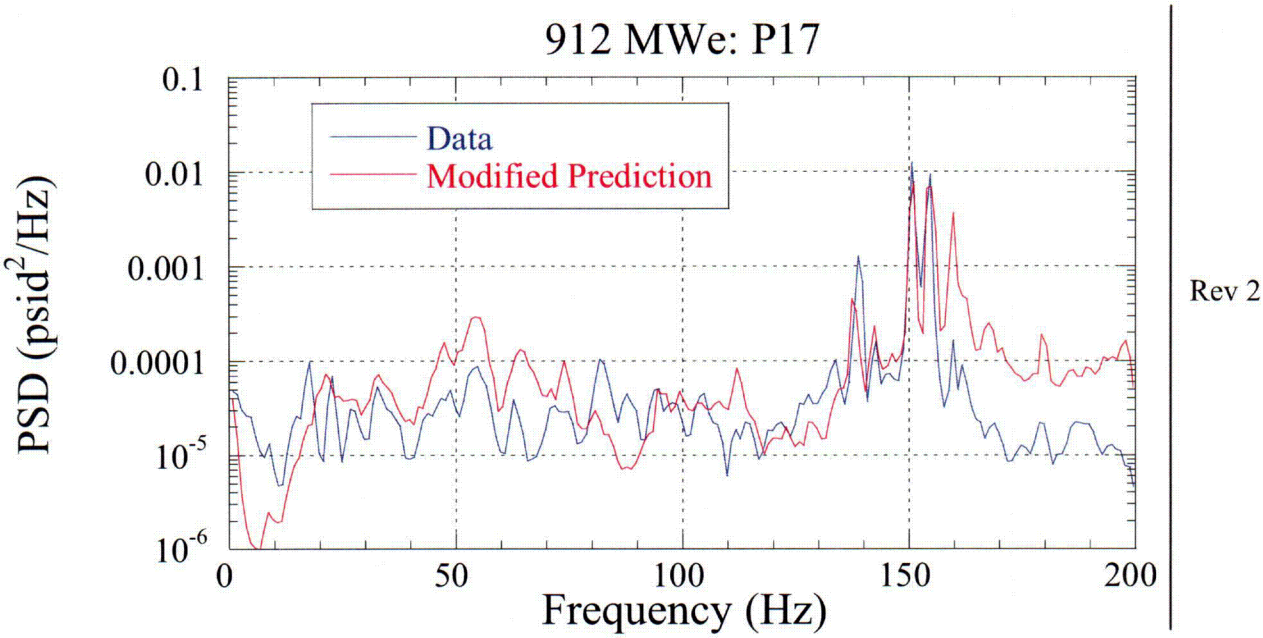

Figure 17. PSD comparison between pressure sensor data (blue curve) and the modified prediction (red curve), for P17.

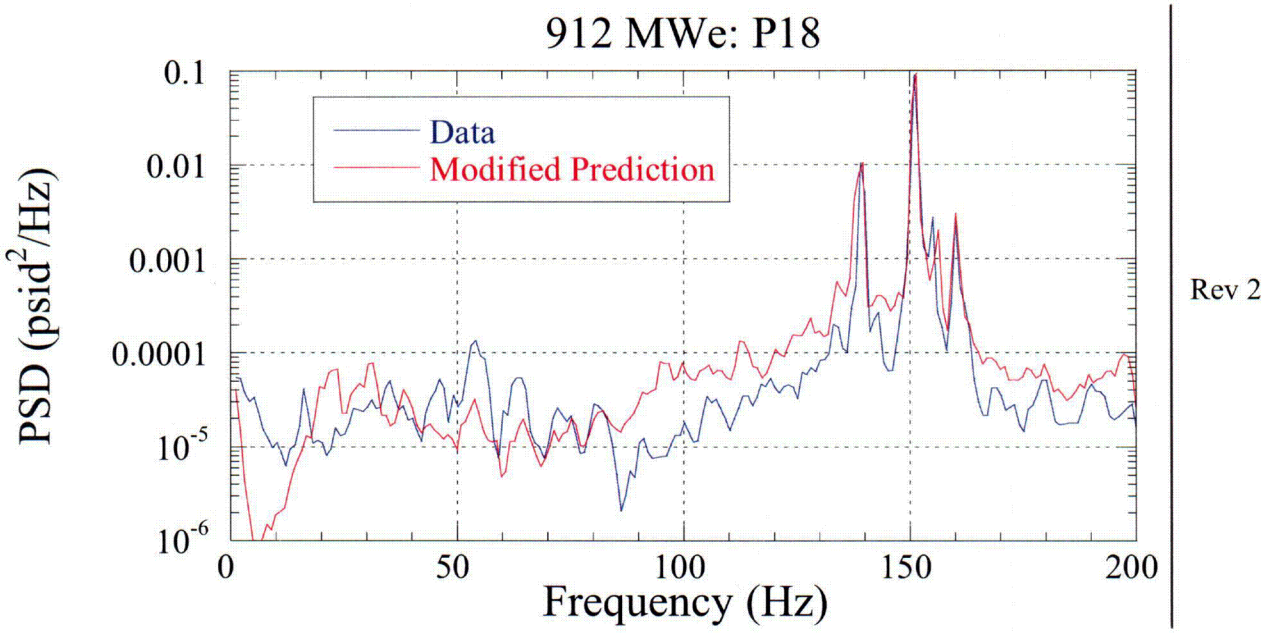

Figure 18. PSD comparison between pressure sensor data (blue curve) and the modified prediction (red curve), for P18.

C09

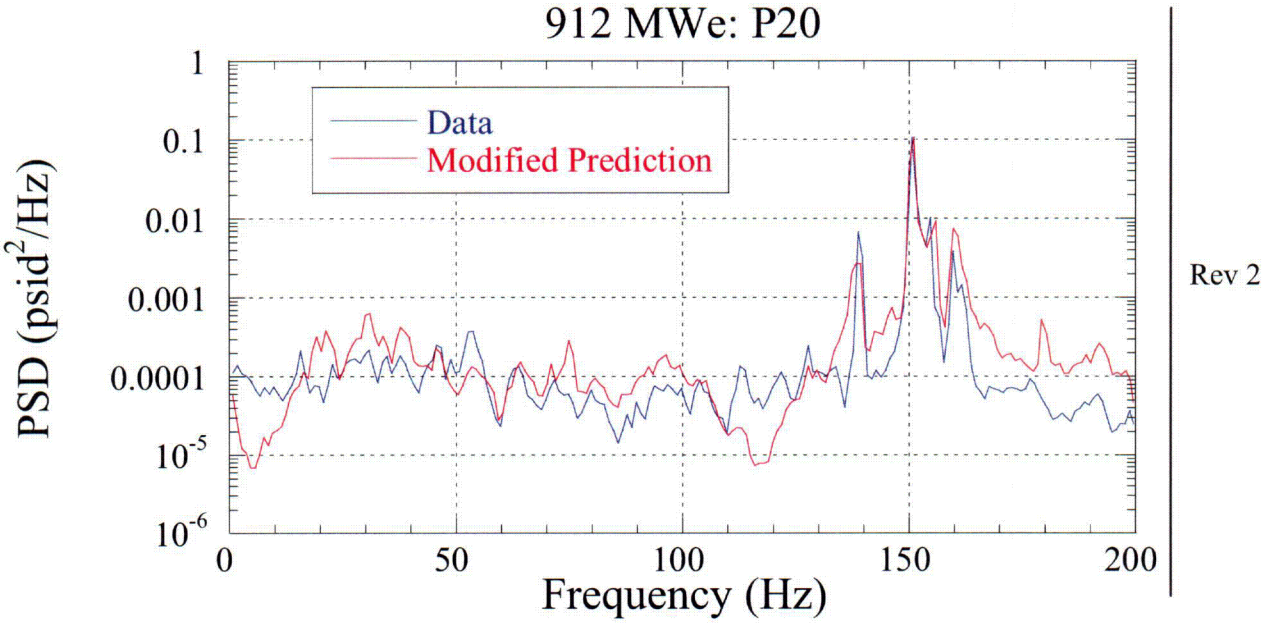

Figure 19. PSD comparison between pressure sensor data (blue curve) and the modified prediction (red curve), for P20.

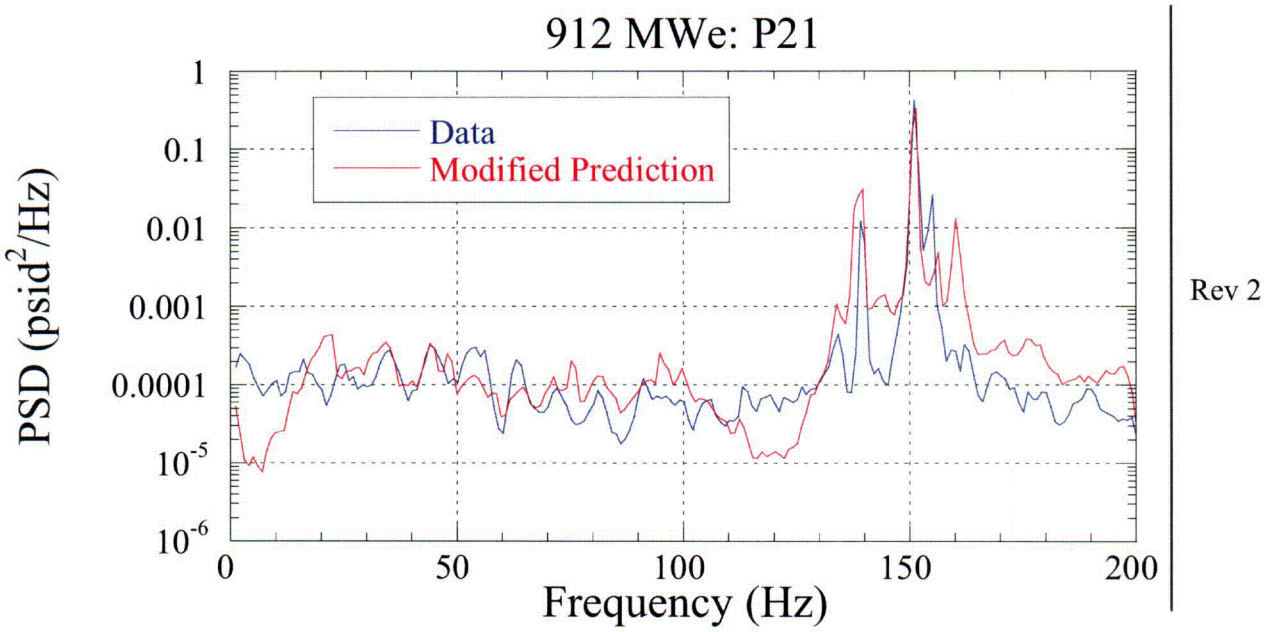

Figure 20. PSD comparison between pressure sensor data (blue curve) and the modified prediction (red curve), for P21.

C10

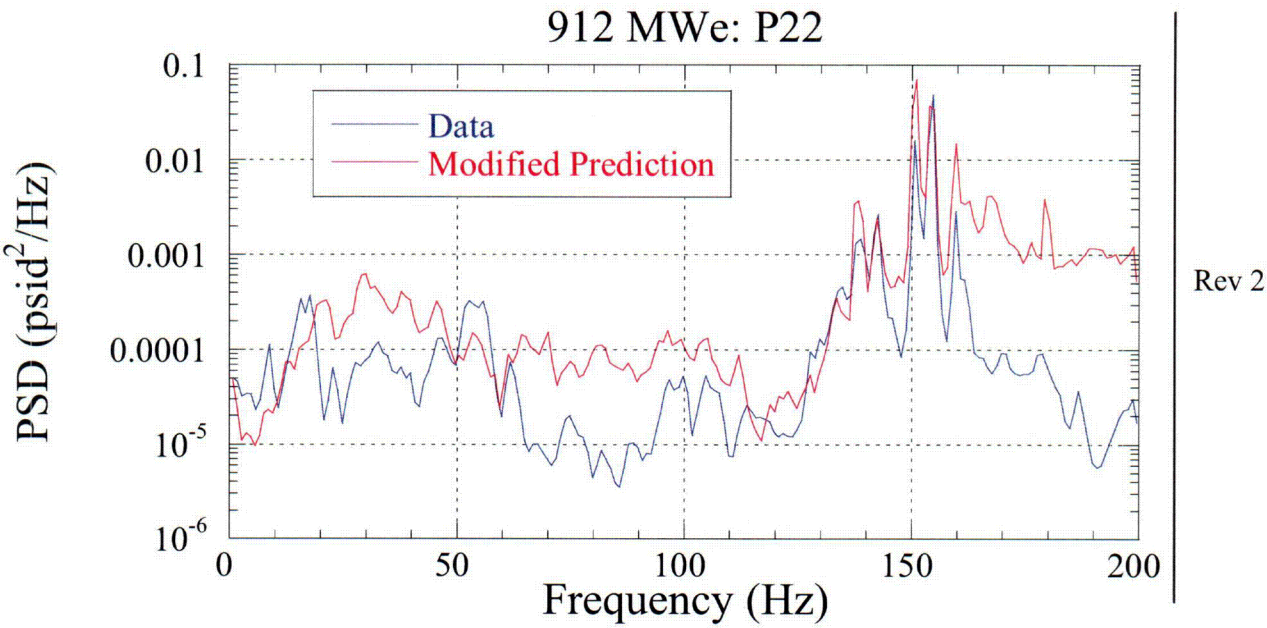

Figure 21. PSD comparison between pressure sensor data (blue curve) and the modified prediction (red curve), for P22.

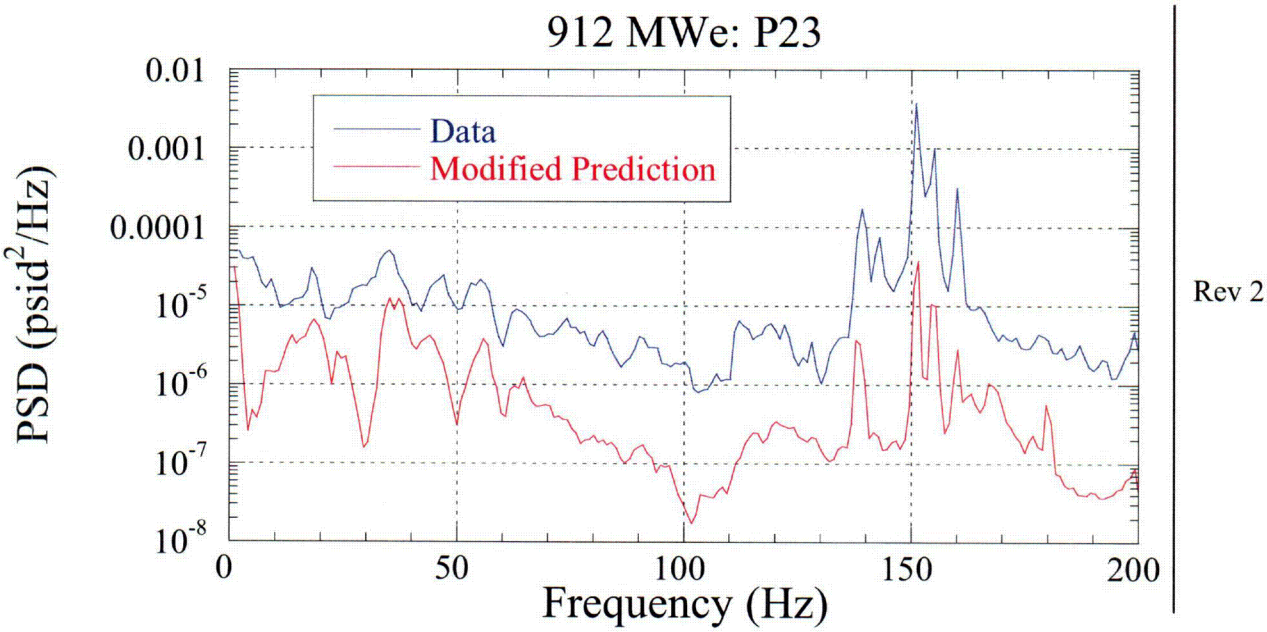

Figure 22. PSD comparison between pressure sensor data (blue curve) and the modified prediction (red curve), for P23 (which is inside the dryer).

C11

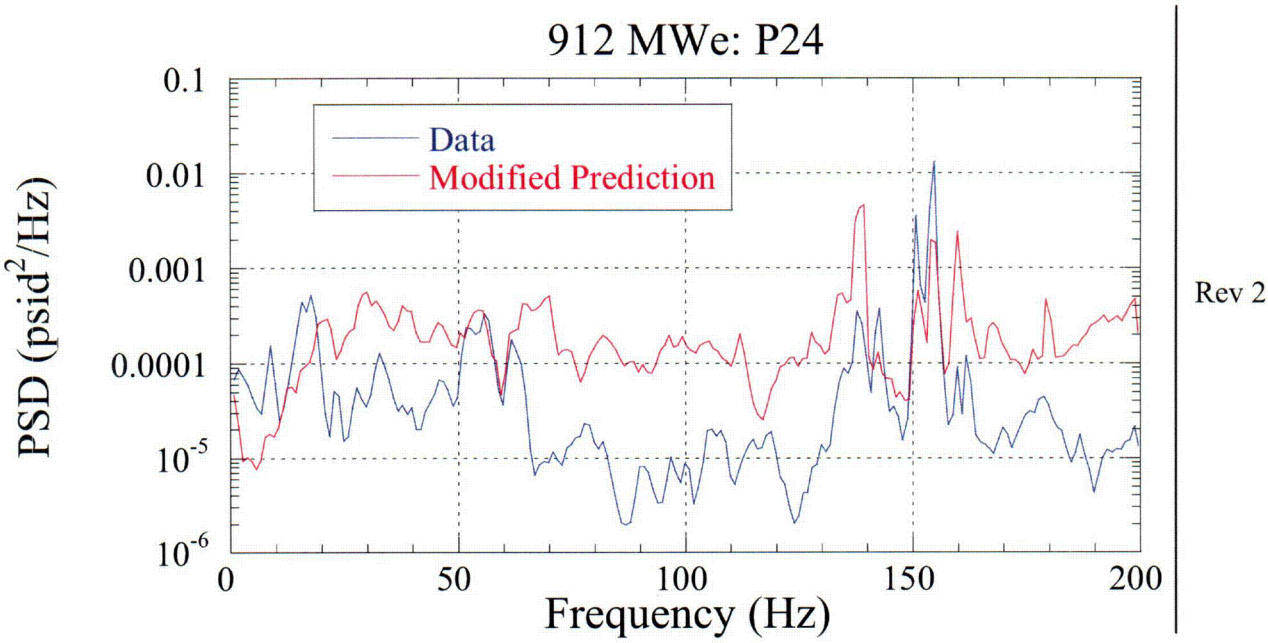

Figure 23. PSD comparison between pressure sensor data (blue curve) and the modified prediction (red curve), for P24.

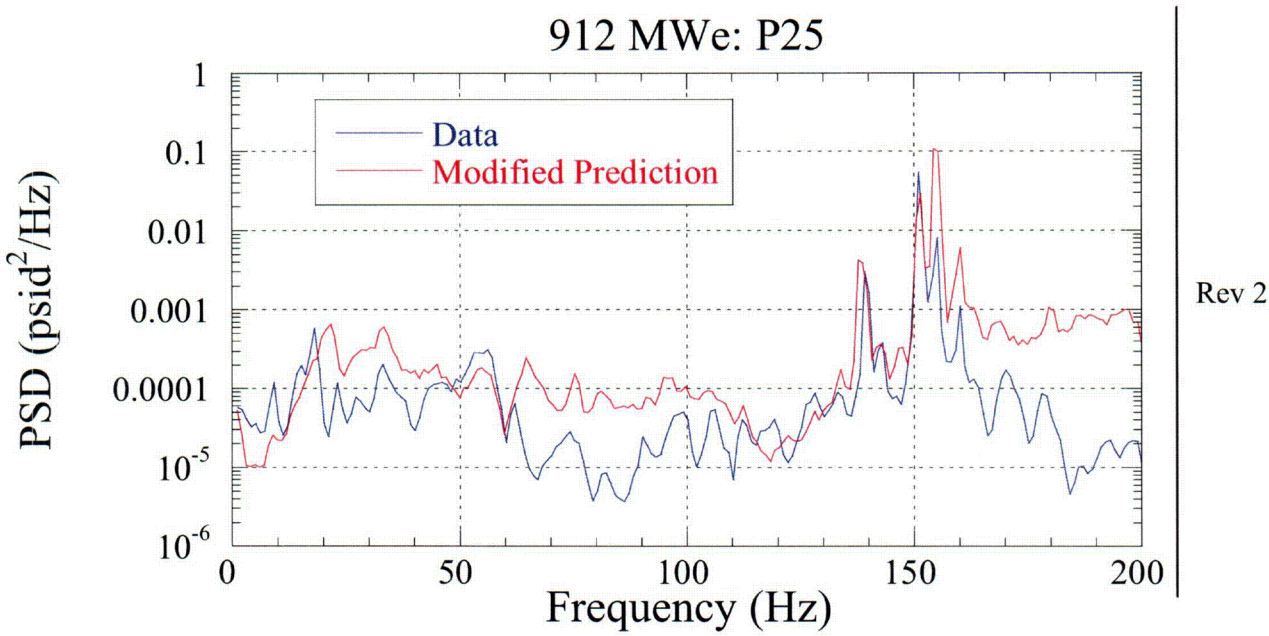

Figure 24. PSD comparison between pressure sensor data (blue curve) and the modified prediction (red curve), for P25.

C12

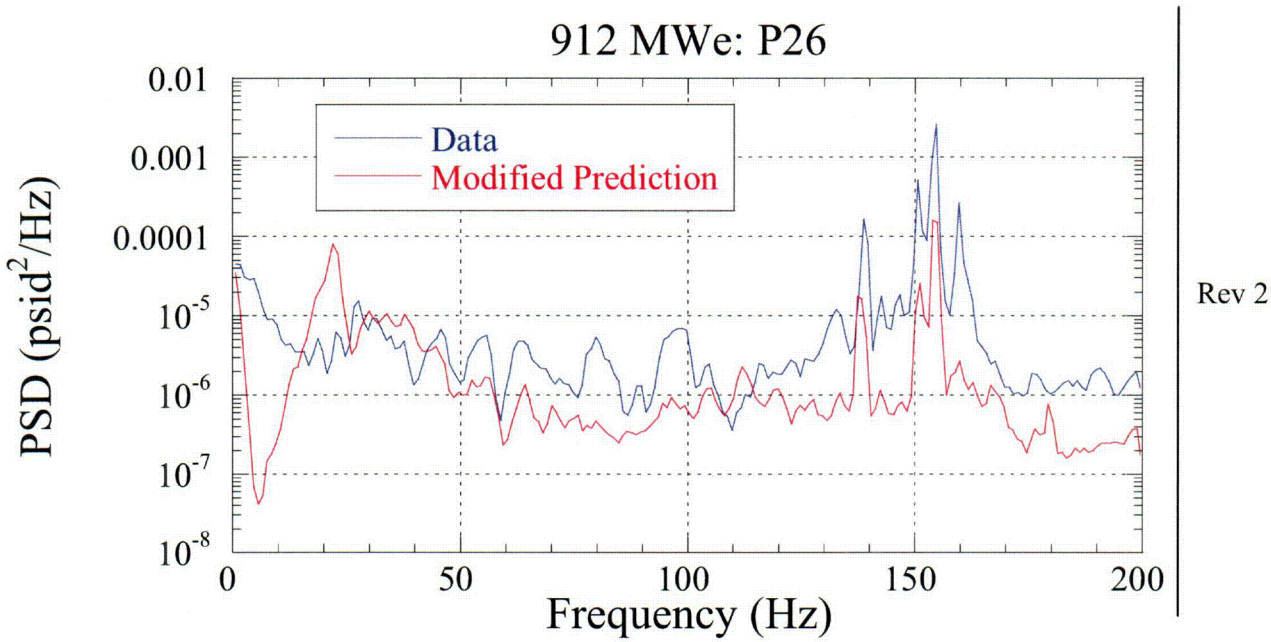

Figure 25. PSD comparison between pressure sensor data (blue curve) and the modified prediction (red curve), for P26.

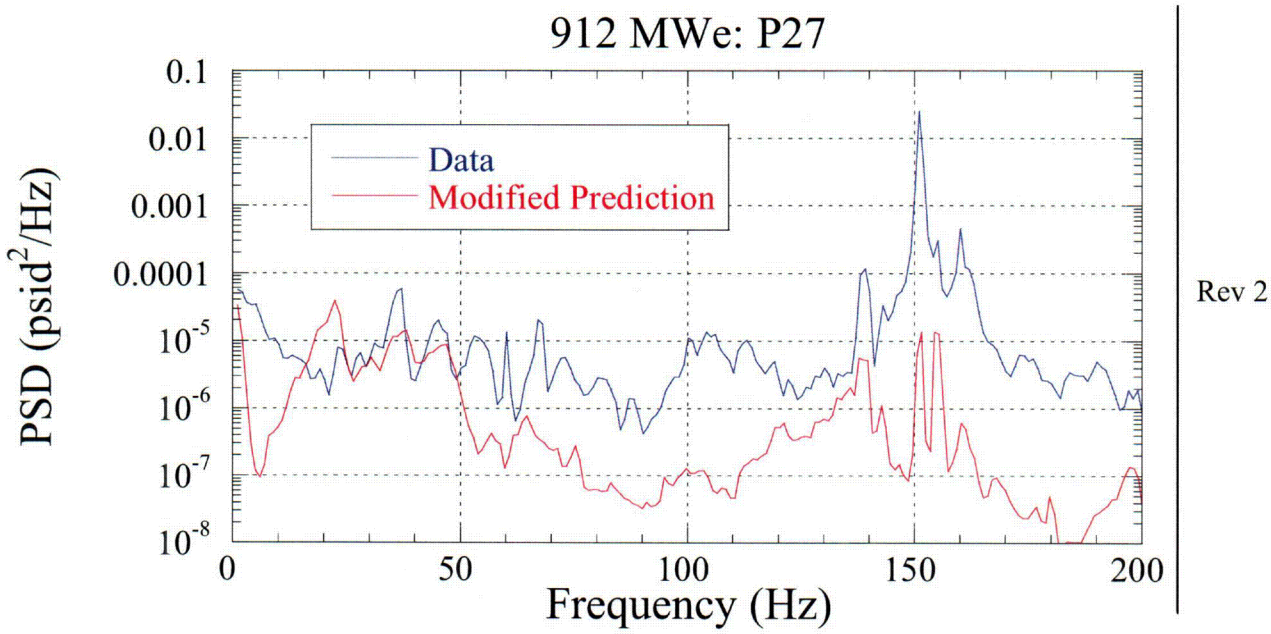

Figure 26. PSD comparison between pressure sensor data (blue curve) and the modified prediction (red curve), for P27 (which is on an inner bank hood).

C13

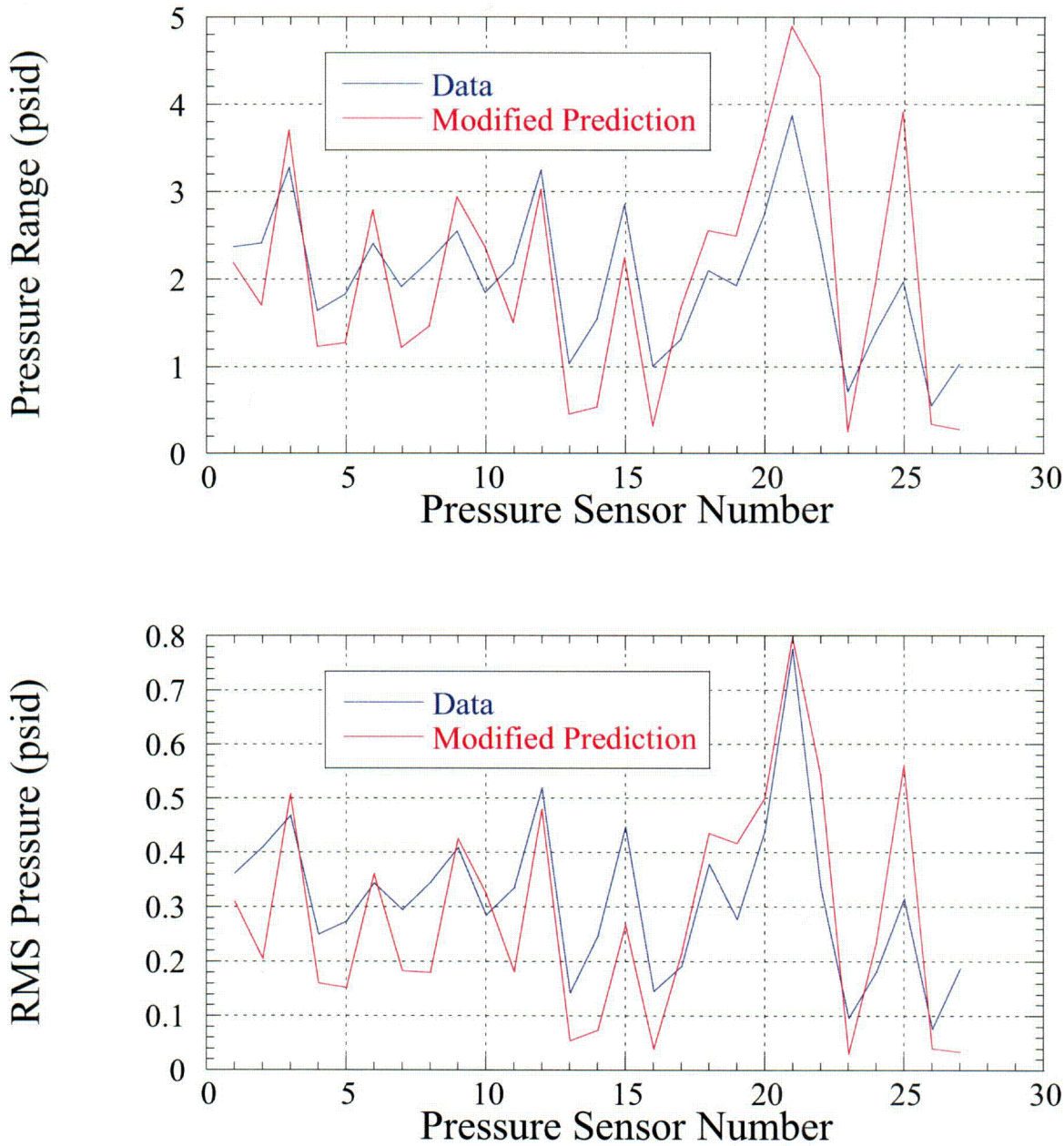

Figure 27. Modified prediction (red curves) compared against the 912 MWe data (blue curves): for pressure range (maximum minus minimum pressures) at all sensors (top) and for RMS pressures at all sensors (bottom). Pressure sensors P13, P14, P16, P23, and P27 are positioned inside the dryer; P19 is inoperative.

C14

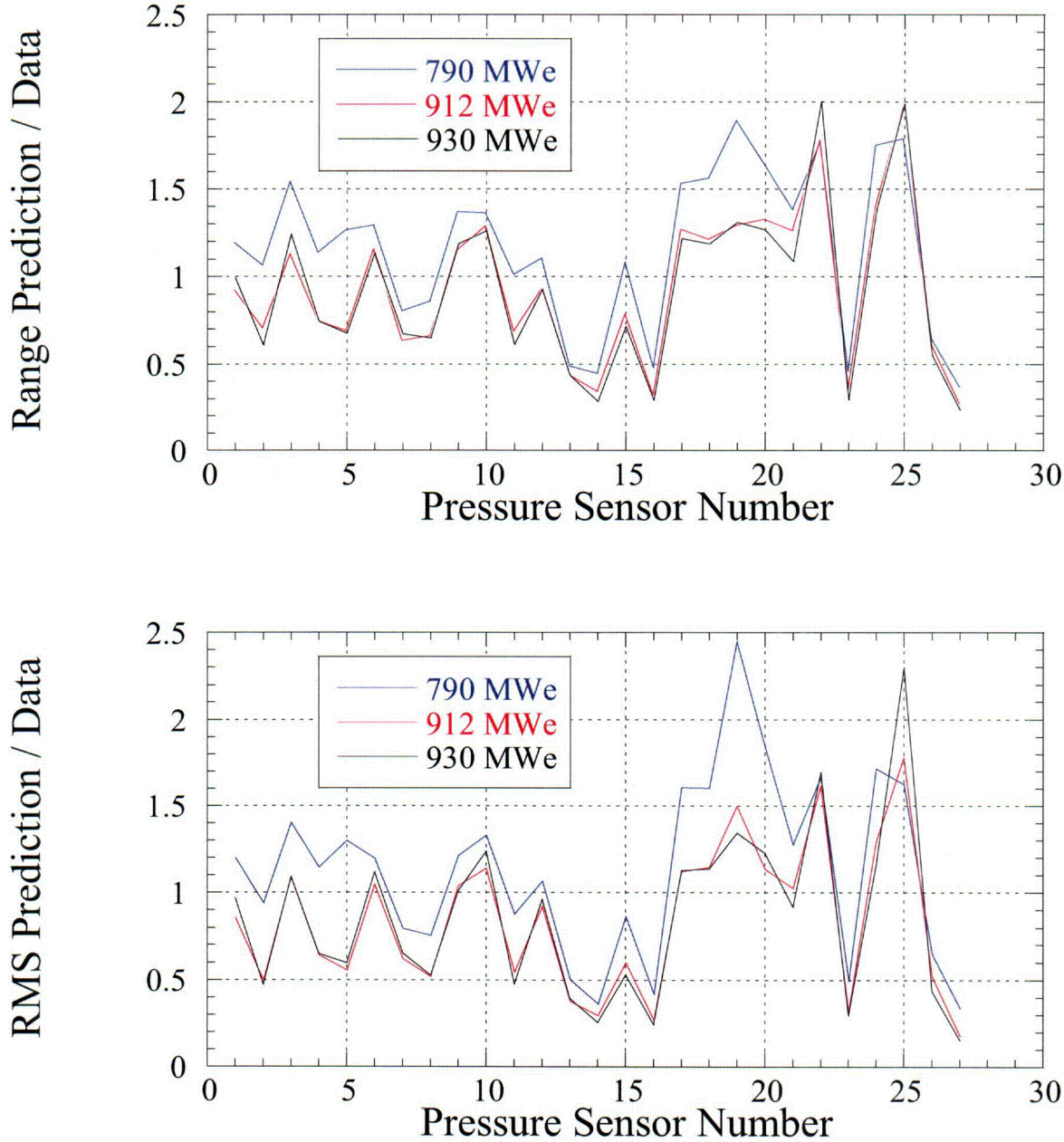

Figure 28. Comparison of the ratio of predicted pressure range divided by the pressure range from data, for all sensors (top), and the ratio of predicted RMS pressure divided by RMS pressure from data, for all sensors (bottom), for 790 MWe (blue curve), 912 MWe (red curve), and 930 MWe (black curve). Values above 1.0 are conservative. Pressure sensors P13, P14, P16, P23, and P27 are positioned inside the dryer; P19 is inoperative.

C15

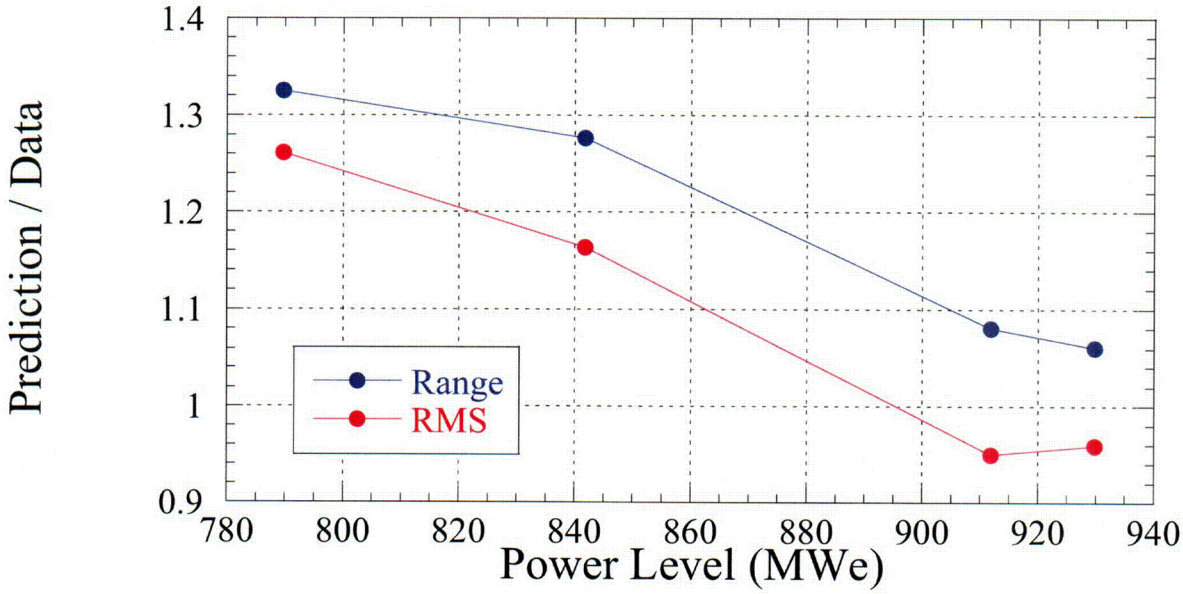

Figure 29. Comparison of the sum of the predictions (external to the dryer) divided by the sum of the measured data (external to the dryer). Pressure range (blue curve); RMS (red curve). Values greater than 1.0 are conservative.

C16